MICROSCOPIC OPTICAL POTENTIAL FROM NN CHIRAL POTENTIALS

Carlotta Giusti
Università and INFN, Pavia

Matteo Vorabbi (TRIUMF)
Paolo Finelli (Bologna)

Nuclear ab initio Theories and Neutrino Physics: INT Seattle February 26 - March 30 2108

OPTICAL POTENTIAL

The OP provides a suitable framework to describe elastic nucleon-nucleus scattering

Its use can be extended to inelastic scattering and to calculate the cross section of a wide variety of nuclear reactions

In our models for QE electron and neutrino-nucleus scattering the OP describes FSI between the emitted nucleon and the residual nucleus

OPTICAL POTENTIAL

PHENOMENOLOGICAL: assume a form and a dependence on a number of adjustable parameters for the real and imaginary parts that characterize the shape of the nuclear density distribution and that vary with the nuclear energy and the nucleus mass number.

Parameters obtained through a fit to pA elastic scattering data

OPTICAL POTENTIAL

PHENOMENOLOGICAL: assume a form and a dependence on a number of adjustable parameters for the real and imaginary parts that characterize the shape of the nuclear density distribution and that vary with the nuclear energy and the nucleus mass number.

Parameters obtained through a fit to pA elastic scattering data

Global OP: the adjustable parameters are fitted in a range of nuclei at many different energies with a dependence of the coefficients in terms of A and E

A independent OP: given for a single target nucleus

OPTICAL POTENTIAL

PHENOMENOLOGICAL: assume a form and a dependence on a number of adjustable parameters for the real and imaginary parts that characterize the shape of the nuclear density distribution and that vary with the nuclear energy and the nucleus mass number.

Parameters obtained through a fit to pA elastic scattering data

THEORETICAL: microscopic calculations require the solution of the full many-body nuclear problem. Some approximations are needed.

We do not expect better description of experimental data (at least for data in the database used to generate phen. OP) but greater predictive power when applied to situations where exp. data not available

OPTICAL POTENTIAL

- Complex
- E dependent
- Non local

M. Vorabbi, P. Finelli, C. Giusti, PRC 93 034619 (2016)

Theoretical optical potential derived from nucleon-nucleon chiral potentials

M. Vorabbi, P. Finelli, C. Giusti, PRC 93 034619 (2017)

Optical potential derived from nucleon-nucleon chiral potentials at N^4LO

M. Vorabbi, P. Finelli, C. Giusti, PRC 93 034619 (2016)

Theoretical optical potential derived from nucleon-nucleon chiral potentials

M. Vorabbi, P. Finelli, C. Giusti, PRC 93 034619 (2017)

Optical potential derived from nucleon-nucleon chiral potentials at N^4LO

PHYSICAL REVIEW VOLUME 89, NUMBER 3 FEBRUARY 1, 1953

Multiple Scattering and the Many-Body Problem—Applications to Photomeson Production in Complex Nuclei*

KENNETH M. WATSON
Physics Department, Indiana University, Bloomington, Indiana
(Received October 1, 1952)

PHYSICAL REVIEW VOLUME 92, NUMBER 2 OCTOBER 15, 1953

The Elastic Scattering of Particles by Atomic Nuclei*

N. C. FRANCIS AND K. M. WATSON†
Department of Physics, Indiana University, Bloomington, Indiana
(Received June 1, 1953)

The Scattering of Fast Nucleons from Nuclei

A. K. Kerman
Massachusetts Institute of Technology, Cambridge, Massachusetts

H. McManus
Chalk River Laboratory, Chalk River, Ontario, Canada

and

R. M. Thaler
Los Alamos Scientific Laboratory, Los Alamos, New Mexico

Received May 27, 1959

M. Vorabbi, P. Finelli, C. Giusti, PRC 93 034619 (2016)

Theoretical optical potential derived from nucleon-nucleon chiral potentials

M. Vorabbi, P. Finelli, C. Giusti, PRC 93 034619 (2017)

Optical potential derived from nucleon-nucleon chiral potentials at N^4LO

Purpose: study the domain of applicability of microscopic two-body chiral potentials to the construction of an OP

M. Vorabbi, P. Finelli, C. Giusti, PRC 93 034619 (2016)

Theoretical optical potential derived from nucleon-nucleon chiral potentials

M. Vorabbi, P. Finelli, C. Giusti, PRC 93 034619 (2017)

Optical potential derived from nucleon-nucleon chiral potentials at N^4LO

Purpose: study the domain of applicability of microscopic two-body chiral potentials to the construction of an OP

Non relativistic optical potential
Comparison with elastic pA scattering data

M. Vorabbi, P. Finelli, C. Giusti, PRC 93 034619 (2016)

Theoretical optical potential derived from nucleon-nucleon chiral potentials

Theoretical framework for pA elastic scattering

We start from the full (A+1) body LS equation

$$T = T + VG_0(E)VT$$

Separation into two coupled integral equations

$$T = U + G_0(E)PT$$

$$U = V + VG_0(E)QU$$

T transition op. for elastic scattering,

U OP

Free propagator	Projection operators	Free Hamiltonian	External interaction
$G_0(E)=(E-H_0+i\epsilon)^{-1}$	$P+Q=1$	$H_0=h_0+H_A$	$V=\sum_{i=1}^{A} v_{0i}$

The spectator expansion

Consistent framework to calculate U and T

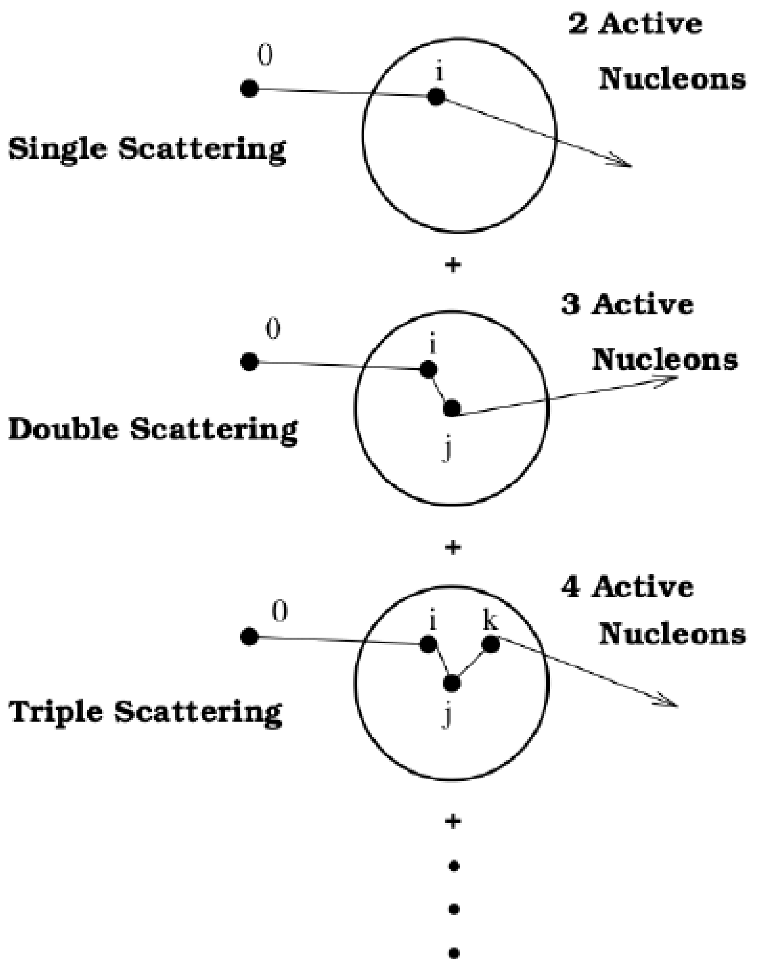

$$U = \sum_{i=1}^{A} \tau_i + \sum_{i,j\neq i}^{A} \tau_{ij} + \sum_{i,j\neq i,k\neq i,j}^{A} \tau_{ijk} + \cdots$$

The spectator expansion

Consistent framework to calculate U and T

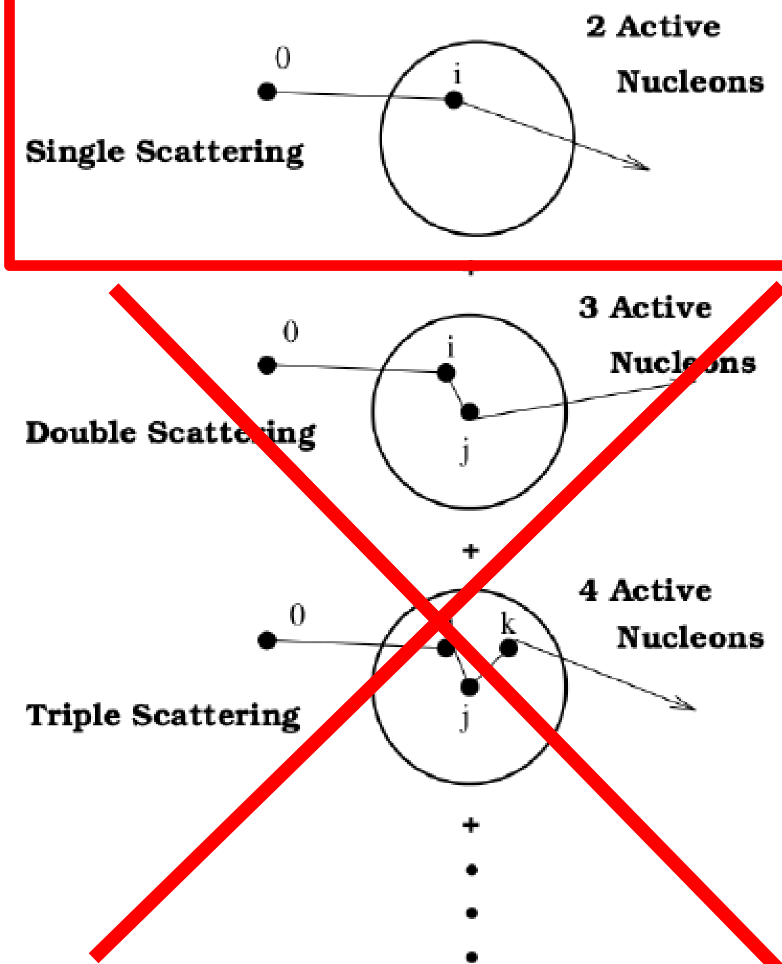

$$U = \sum_{i=1}^{A} \tau_i + \sum_{i,j\neq i}^{A} \tau_{ij} + \sum_{i,j\neq i,k\neq i,j}^{A} \tau_{ijk} + \cdots$$

The spectator expansion

Consistent framework to calculate U and T

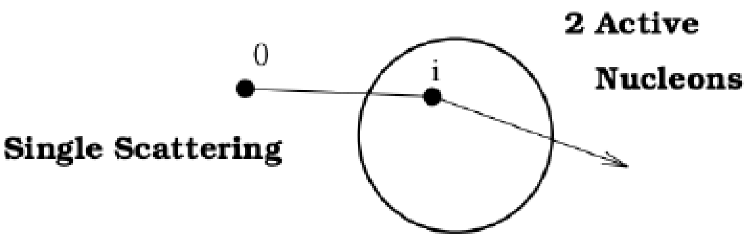

$$U = \sum_{i=1}^{A} \tau_i$$

$$\tau_i = v_{0i} + v_{0i} G_0(E) Q \tau_i$$

Impulse Approximation

$$\tau_i \approx t_{0i}$$

The free NN t matrix

$$t_{0i} = v_{0i} + v_{0i} g_i t_{0i}$$

The free two-body propagator

$$g_i = \frac{1}{E - h_0 - h_i + i\epsilon}$$

$$U = \sum_{i=1}^{A} t_{0i}$$

Impulse Approximation

$$\tau_i \approx t_{0i}$$

The free NN t matrix

$$t_{0i} = v_{0i} + v_{0i} g_i t_{0i}$$

The free two-body propagator

$$g_i = \frac{1}{E - h_0 - h_i + i\epsilon}$$

$$U = \sum_{i=1}^{A} t_{0i}$$

We have to solve only 2-body equations

Optimum Factorization Approximation

$$U(\boldsymbol{q},\boldsymbol{K};\omega) = \frac{A-1}{A}\,\eta(\boldsymbol{q},\boldsymbol{K}) \sum_{N=n,p} t_{pN}\left[\boldsymbol{q},\frac{A+1}{A}\boldsymbol{K};\omega\right] \rho_N(q)$$

NN t-matrix
NN interaction

n, p densities

$\boldsymbol{q}=\boldsymbol{k}'-\boldsymbol{k}$ $\qquad$ $\boldsymbol{K}=\frac{1}{2}(\boldsymbol{k}'+\boldsymbol{k})$

Optimum Factorization Approximation

$$U(q, \boldsymbol{K}; \omega) = \frac{A-1}{A} \eta(q, \boldsymbol{K}) \sum_{N=n,p} t_{pN} \left[q, \frac{A+1}{A} \boldsymbol{K}; \omega \right] \rho_N(q)$$

Moeller factor
imposes the Lorentz invariance of the flux when passing from the NA to the NN frame in which the t matrices are evaluated

$$U(q, K; \omega) = U^c(q, K; \omega) + \frac{i}{2}\sigma \cdot q \times K\, U^{ls}(q, K; \omega)$$

central spin-orbit

$$U^c(q, K; \omega) = \frac{A-1}{A}\,\eta(q, K) \sum_{N=n,p} t^c_{pN}\left[q, \frac{A+1}{A}K; \omega\right] \rho_N(q)$$

$$U^{ls}(q, K; \omega) = \frac{A-1}{A}\,\eta(q, K)\frac{A+1}{2A} \sum_{N=n,p} t^{ls}_{pN}\left[q, \frac{A+1}{A}K; \omega\right] \rho_N(q)$$

$$U(q,K;\omega) = U^c(q,K;\omega) + \frac{i}{2}\sigma\cdot q\times K\, U^{ls}(q,K;\omega)$$

central   spin-orbit

$$U^c(q,K;\omega) = \frac{A-1}{A}\eta(q,K) \sum_{N=n,p} t^c_{pN}\left[q,\frac{A+1}{A}K;\omega\right]\rho_N(q)$$

$$U^{ls}(q,K;\omega) = \frac{A-1}{A}\eta(q,K)\frac{A+1}{2A} \sum_{N=n,p} t^{ls}_{pN}\left[q,\frac{A+1}{A}K;\omega\right]\rho_N(q)$$

NN t-matrix
NN interaction

n, p densities

Optimum Factorization Approximation

$$U(\boldsymbol{q},\boldsymbol{K};\omega)=\frac{A-1}{A}\,\eta(\boldsymbol{q},\boldsymbol{K})\sum_{N=n,p} t_{pN}\left[\boldsymbol{q},\frac{A+1}{A}\boldsymbol{K};\omega\right]\ \rho_N(\boldsymbol{q})$$

Moeller factor

NN t-matrix
NN interaction

n, p densities

- n,p densities calculated within the RMF description of spherical nuclei using a DDME model
- NN interaction chiral potentials...

CHIRAL POTENTIAL

- When the concept of EFT was applied to low-energy QCD, ChPT was developed
- Within ChPT it became possible to implement chiral symmetry consistently in a theory of pionic and nuclear interactions
- The theory is based on a perturbative expansion in powers of $(Q/\Lambda_\chi)^n$ where Q is the magnitude of the three-momentum of the external particles or the pion mass and Λ_χ is the chiral symmetry breaking scale of the chiral EFT
- From the perturbative expansion only a finite number of terms contribute at a given order

CHIRAL POTENTIAL

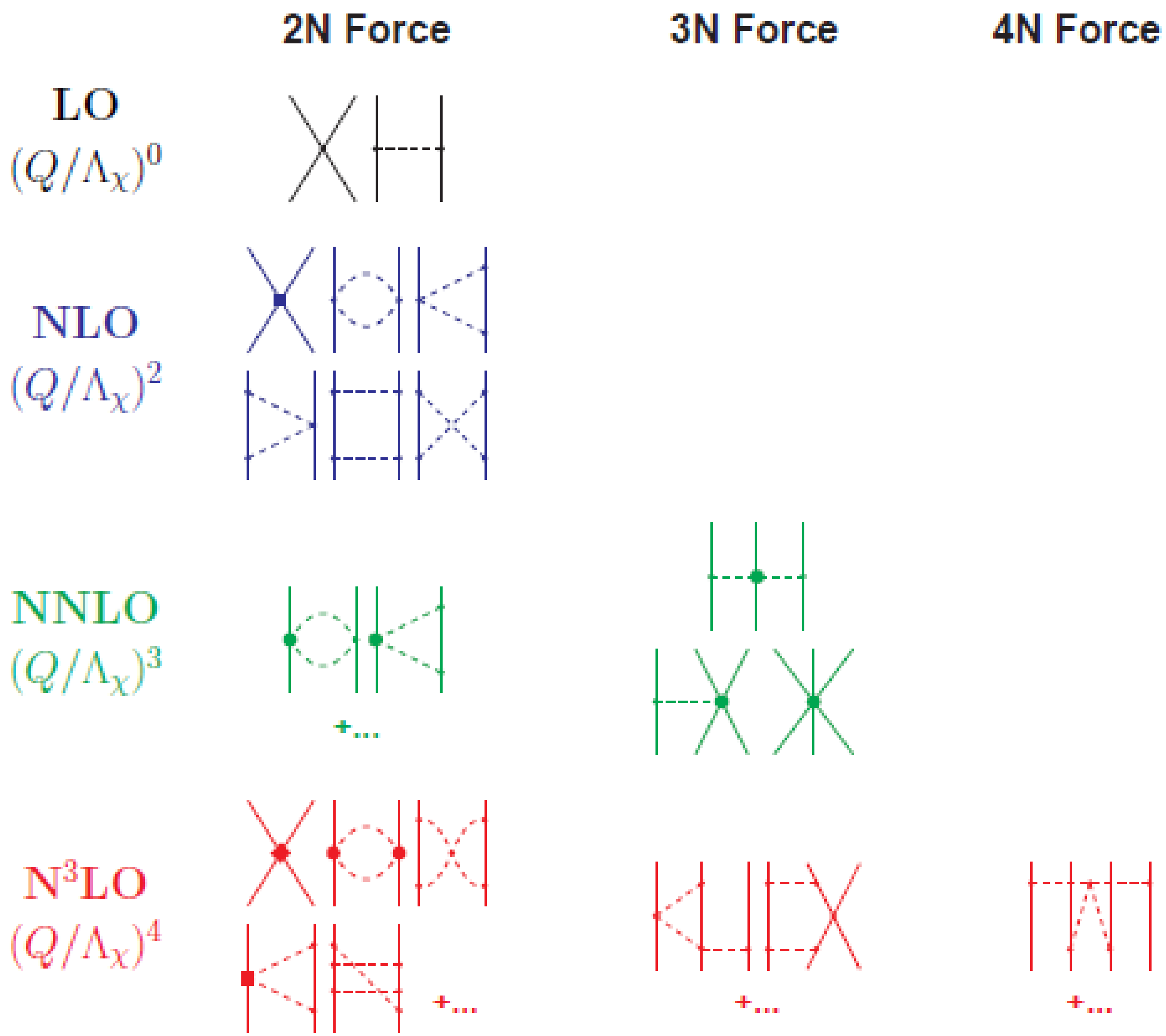

CHIRAL POTENTIAL

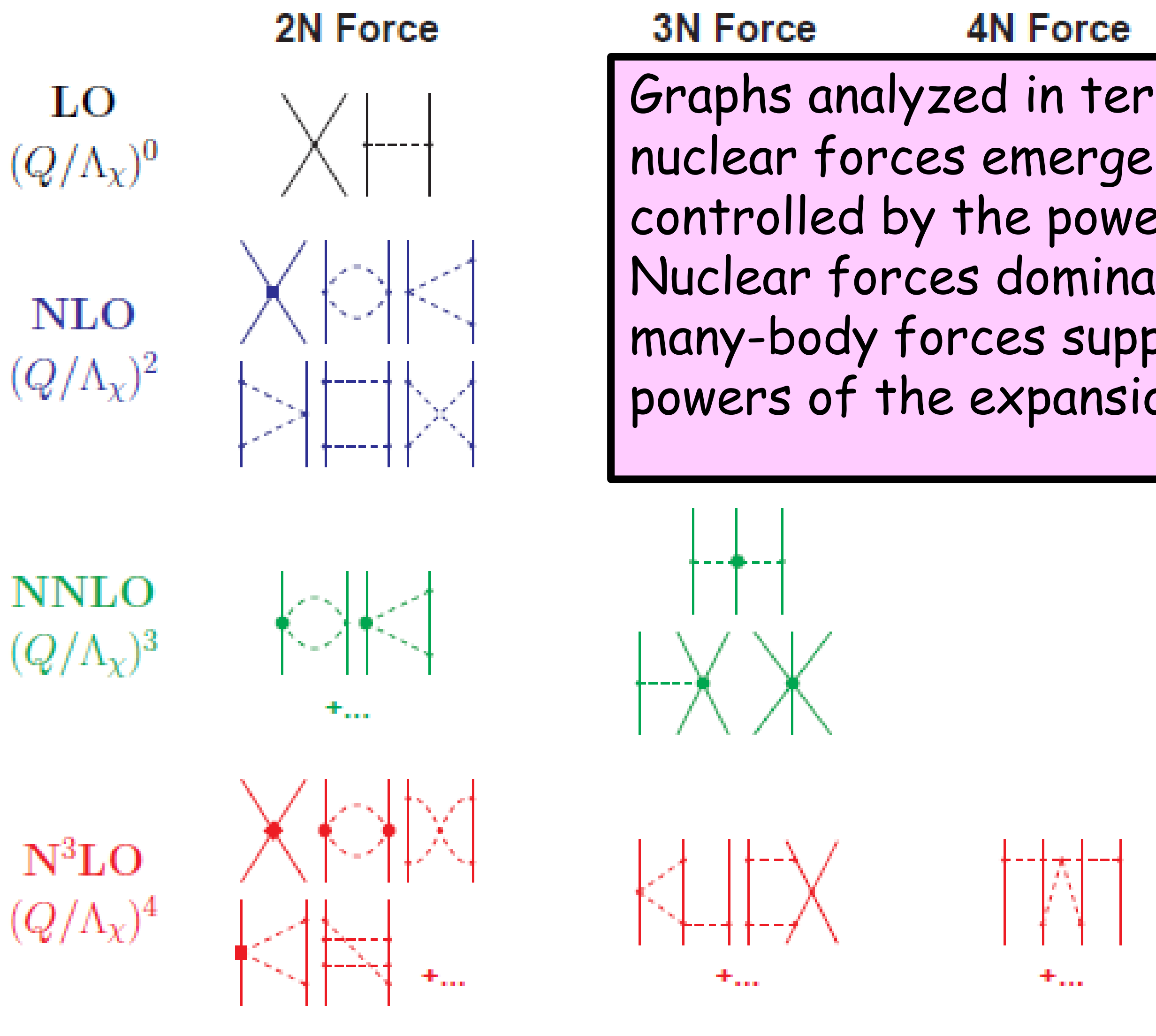

Graphs analyzed in terms of $(Q/\Lambda_\chi)^n$
nuclear forces emerge as a hierarchy
controlled by the power n
Nuclear forces dominated by NN int.
many-body forces suppressed by
powers of the expansion parameters.

CHIRAL POTENTIAL

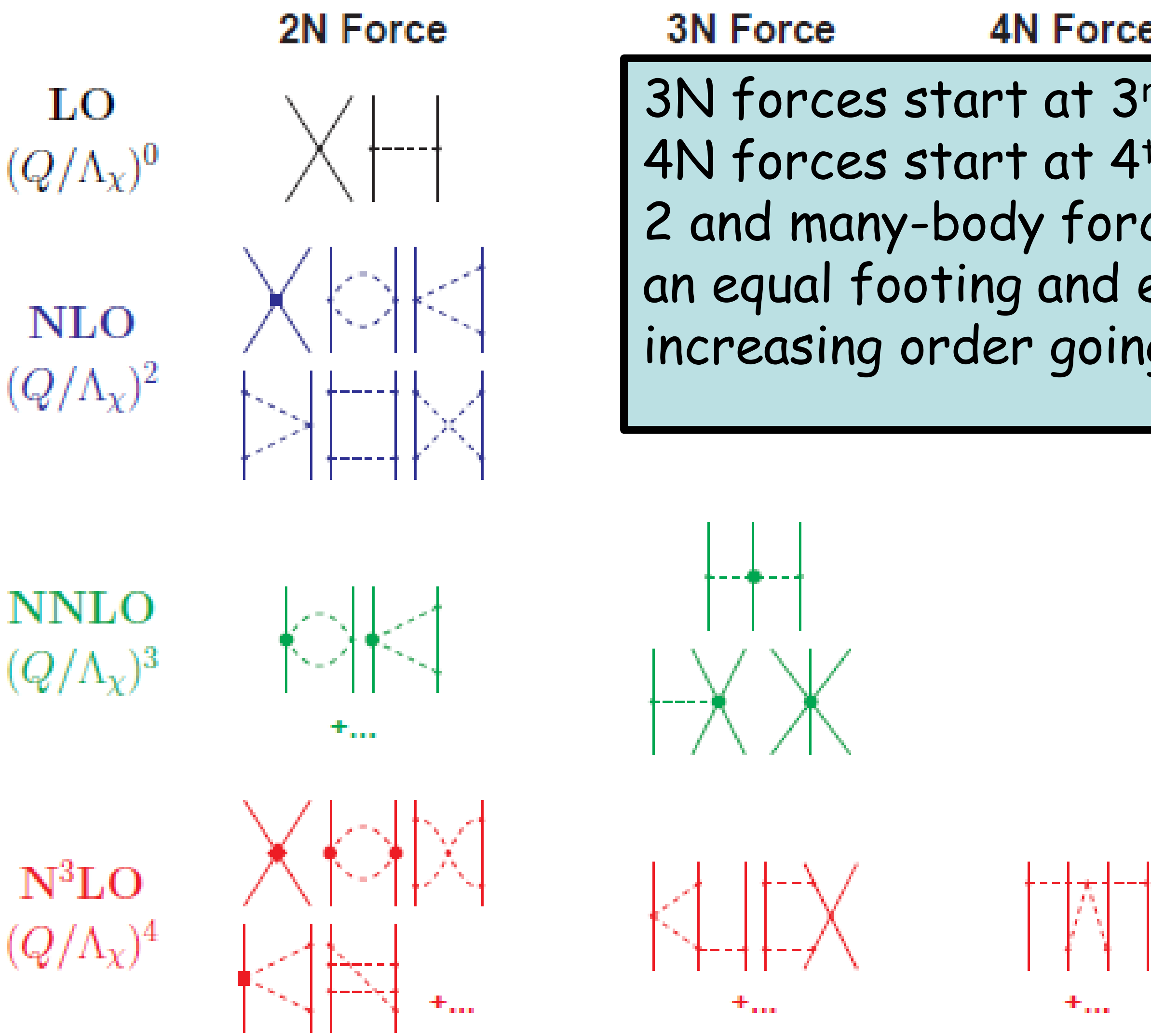

3N forces start at 3rd order,
4N forces start at 4th order
2 and many-body forces are created on an equal footing and emerge in increasing order going to higher order

CHIRAL POTENTIAL

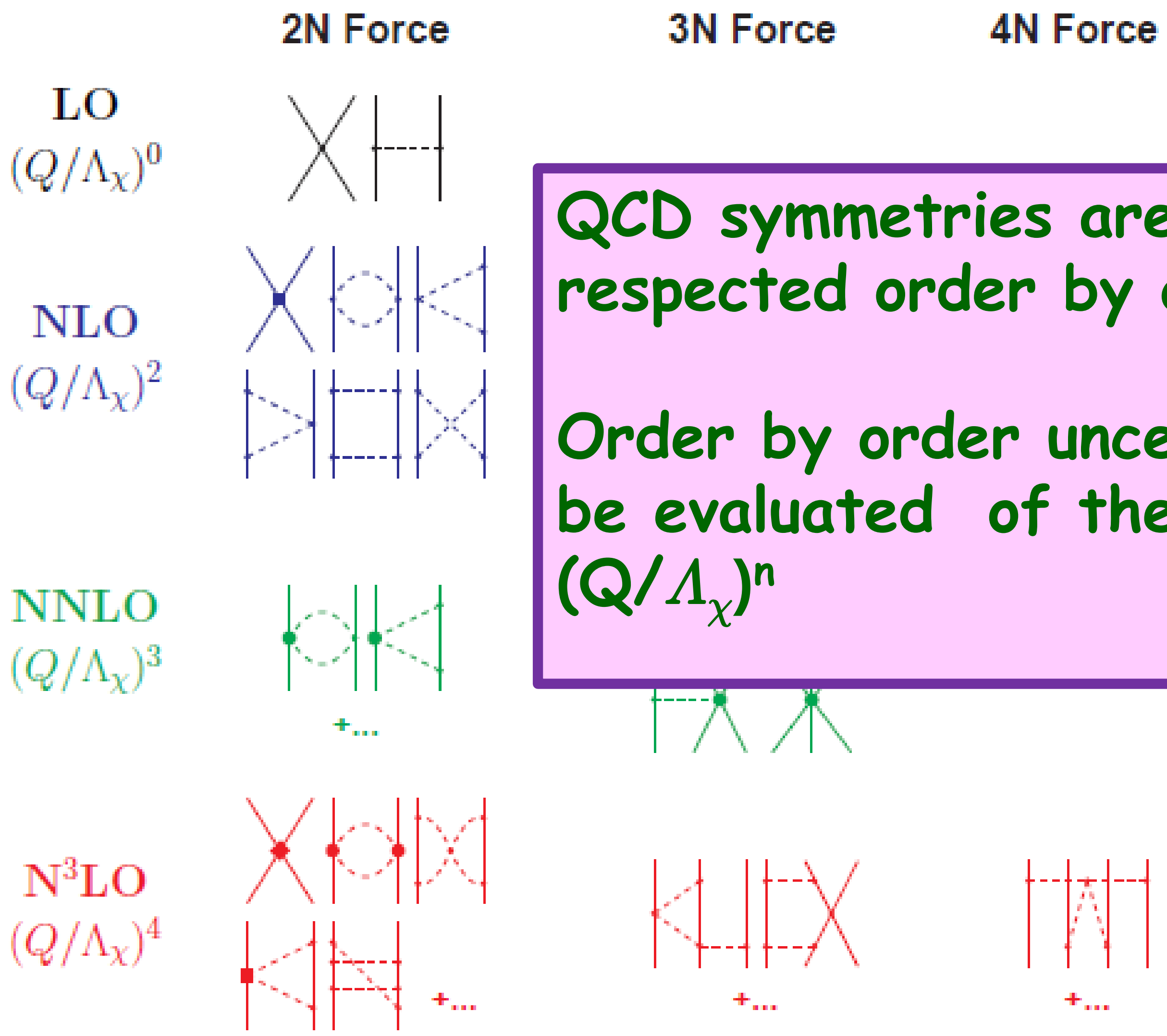

QCD symmetries are consistently respected order by order

Order by order uncertainties can be evaluated of the order $(Q/\Lambda_\chi)^n$

CHIRAL POTENTIAL

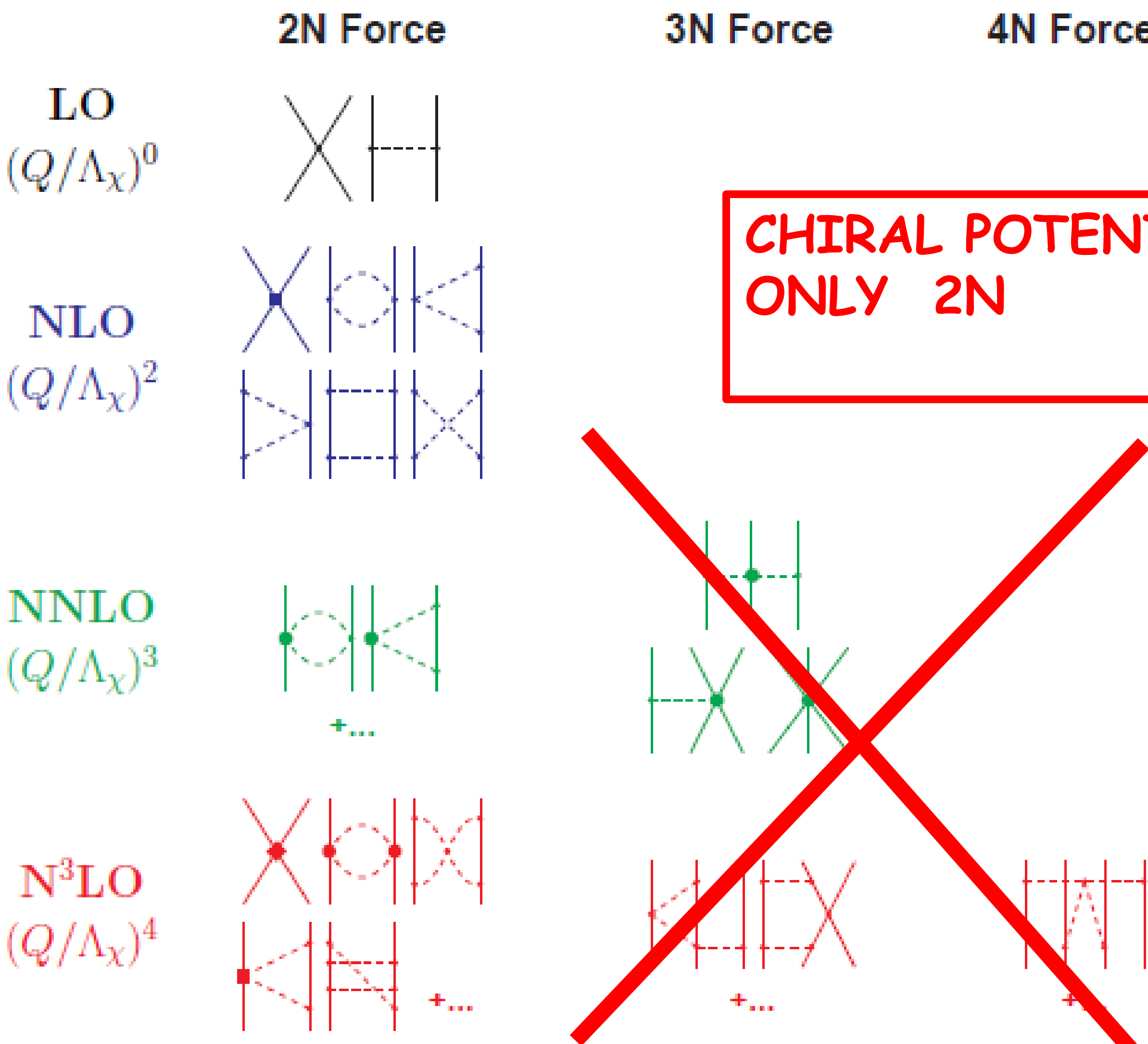

CHIRAL POTENTIAL AT N^{3}LO
ONLY 2N

CHIRAL POTENTIAL

Two different versions of chiral potentials at N^3LO
Entem and Machledt (EM) , Epelbaum et al. (EGM)

In general the integral in the LS eq . is divergent and needs to be regularized

Usual procedure: $$V(k',k) \longmapsto V(k',k)\, e^{-(k'/\Lambda)^{2n}}\, e^{-(k/\Lambda)^{2n}}$$

EM present results with Λ = 450, 500, 600 MeV
EGM present results with Λ = 450, 550, 600 MeV
and treat differently the short-range part of the 2PE contribution, that has an unphysically strong attraction.
EM dimensional regularization
EGM spectral function regularization introduces an additional cutoff $\tilde{\Lambda}$ and give cut-off combinations: (Λ, $\tilde{\Lambda}$) = (450,500), (450,700), (550,600), (600,600), (600,700)

CHIRAL POTENTIAL

Two different versions of chiral potentials at N^{3}LO
Entem and Machledt (EM) , Epelbaum et al. (EGM)

In general the integral in the LS eq . is divergent and needs to be regularized

Usual procedure: $$V(k',k) \longmapsto V(k',k)\, e^{-(k'/\Lambda)^{2n}}\, e^{-(k/\Lambda)^{2n}}$$

EM present results with Λ = 450, 500, 600 MeV
EGM present results with Λ = 450, 550, 600 MeV
and treat differently the short-range part of the 2PE contribution, that has an unphysically strong attraction.
EM dimensional regularization
EGM spectral function regularization introduces an additional cutoff $\tilde{\Lambda}$ and give cut-off combinations: (Λ, $\tilde{\Lambda}$) = (450,500), (450,700), (550,600), (600,600), (600,700)

sensitivity to the cutoff parameters
order by order convergence

NN transition matrix

NN elastic scatt. amplitude related to the antisymmetrized NN-t matrix elements

$$M(\boldsymbol{\kappa}', \boldsymbol{\kappa}, \omega) = \langle \boldsymbol{\kappa}' | M(\omega) | \boldsymbol{\kappa} \rangle = -4\pi^2 \mu \langle \boldsymbol{\kappa}' | t(\omega) | \boldsymbol{\kappa} \rangle$$

The most general form , consistent with invariance under rotation, time reversal, and parity

$$M = a + c(\boldsymbol{\sigma}_1 + \boldsymbol{\sigma}_2) \cdot \hat{\boldsymbol{n}} + m(\boldsymbol{\sigma}_1 \cdot \hat{\boldsymbol{n}})(\boldsymbol{\sigma}_2 \cdot \hat{\boldsymbol{n}})$$

$$+ (g + h)(\boldsymbol{\sigma}_1 \cdot \hat{\boldsymbol{l}})(\boldsymbol{\sigma}_2 \cdot \hat{\boldsymbol{l}}) + (g - h)(\boldsymbol{\sigma}_1 \cdot \hat{\boldsymbol{m}})(\boldsymbol{\sigma}_2 \cdot \hat{\boldsymbol{m}})$$

$$\hat{l} = \frac{\kappa' + \kappa}{|\kappa' + \kappa|}, \qquad \hat{m} = \frac{\kappa' - \kappa}{|\kappa' - \kappa|}, \qquad \hat{n} = \frac{\kappa \times \kappa'}{|\kappa \times \kappa'|}$$

a, c, m, g, h complex functions of ω, κ, κ'

NN transition matrix

NN elastic scatt. amplitude related to the antisymmetrized NN-t matrix elements

$$M(\boldsymbol{\kappa}', \boldsymbol{\kappa}, \omega) = \langle \boldsymbol{\kappa}' | M(\omega) | \boldsymbol{\kappa} \rangle = -4\pi^2 \mu \langle \boldsymbol{\kappa}' | t(\omega) | \boldsymbol{\kappa} \rangle$$

The most general form , consistent with invariance under rotation, time reversal, and parity

$$M = a + c(\boldsymbol{\sigma}_1 + \boldsymbol{\sigma}_2) \cdot \hat{\boldsymbol{n}} + m(\boldsymbol{\sigma}_1 \cdot \hat{\boldsymbol{n}})(\boldsymbol{\sigma}_2 \cdot \hat{\boldsymbol{n}})$$
$$+ (g + h)(\boldsymbol{\sigma}_1 \cdot \hat{\boldsymbol{l}})(\boldsymbol{\sigma}_2 \cdot \hat{\boldsymbol{l}}) + (g - h)(\boldsymbol{\sigma}_1 \cdot \hat{\boldsymbol{m}})(\boldsymbol{\sigma}_2 \cdot \hat{\boldsymbol{m}})$$

$$\hat{l} = \frac{\kappa' + \kappa}{|\kappa' + \kappa|}, \qquad \hat{m} = \frac{\kappa' - \kappa}{|\kappa' - \kappa|}, \qquad \hat{n} = \frac{\kappa \times \kappa'}{|\kappa \times \kappa'|}$$

a, c, m, g, h complex functions of ω, κ, κ'

For even-even nuclei with J=0 only a and c survive and they are connected to the central and spin-orbit part of the NN t-matrix

THE NUCLEON-NUCLEON AMPLITUDES

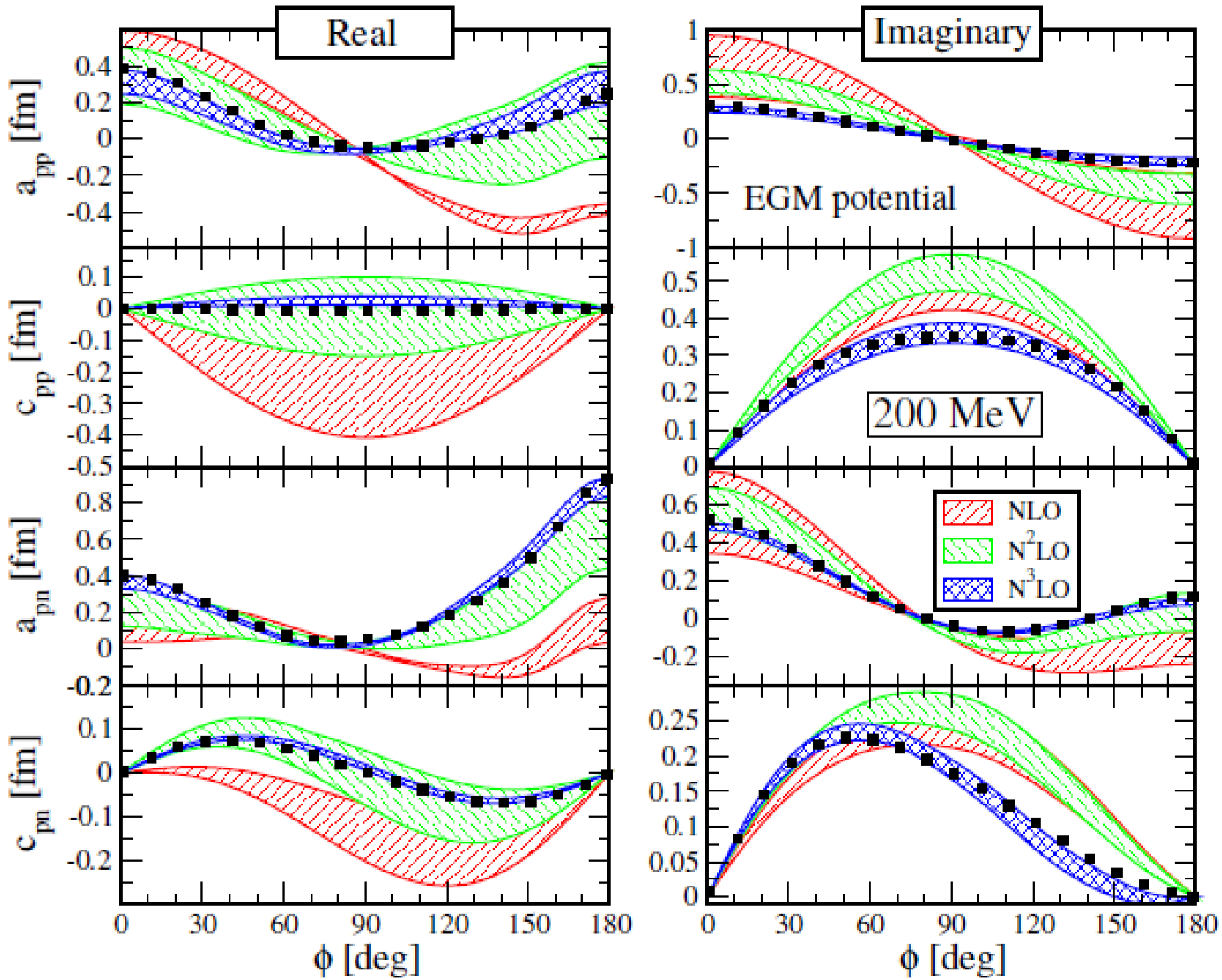

M. Vorabbi, P. Finelli, and C. Giusti, Phys. Rev. C **93**, 034619 (2016)

NN AMPLITUDES 200 MeV

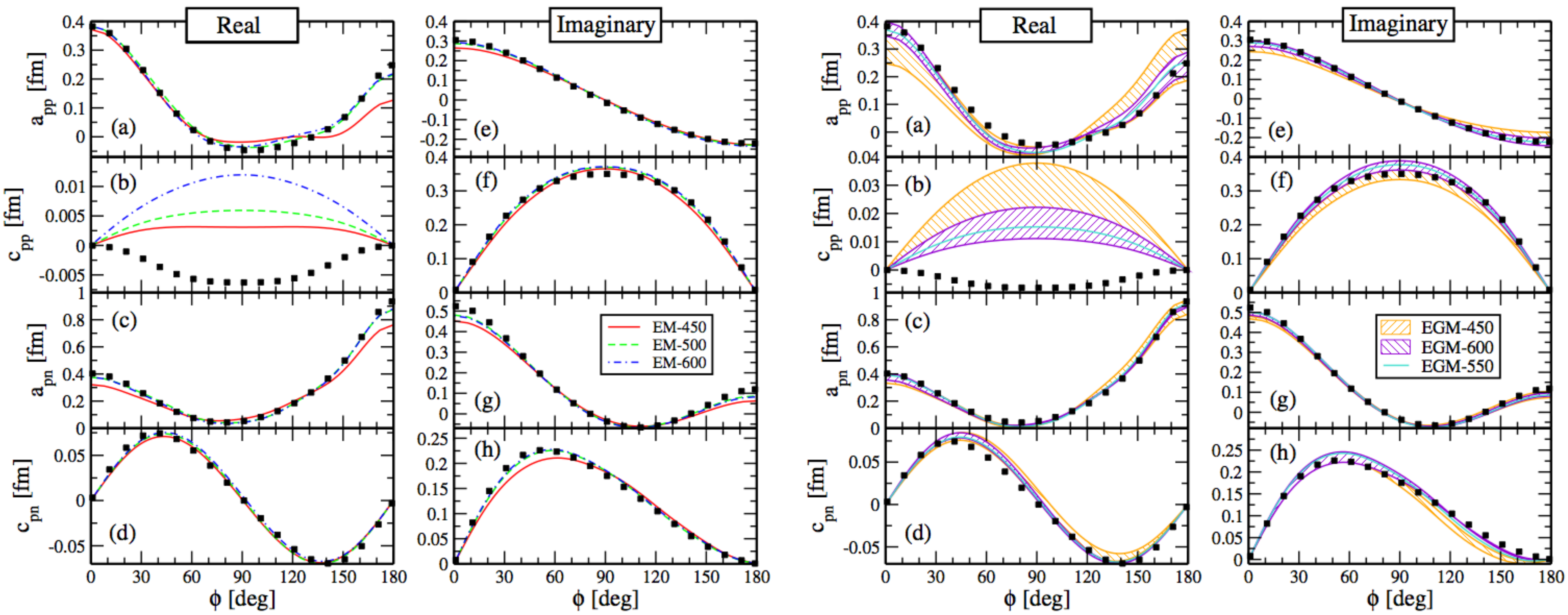

M. Vorabbi, P. Finelli, C. Giusti, PRC 93 034619 (2016)

NN AMPLITUDES 100 MeV

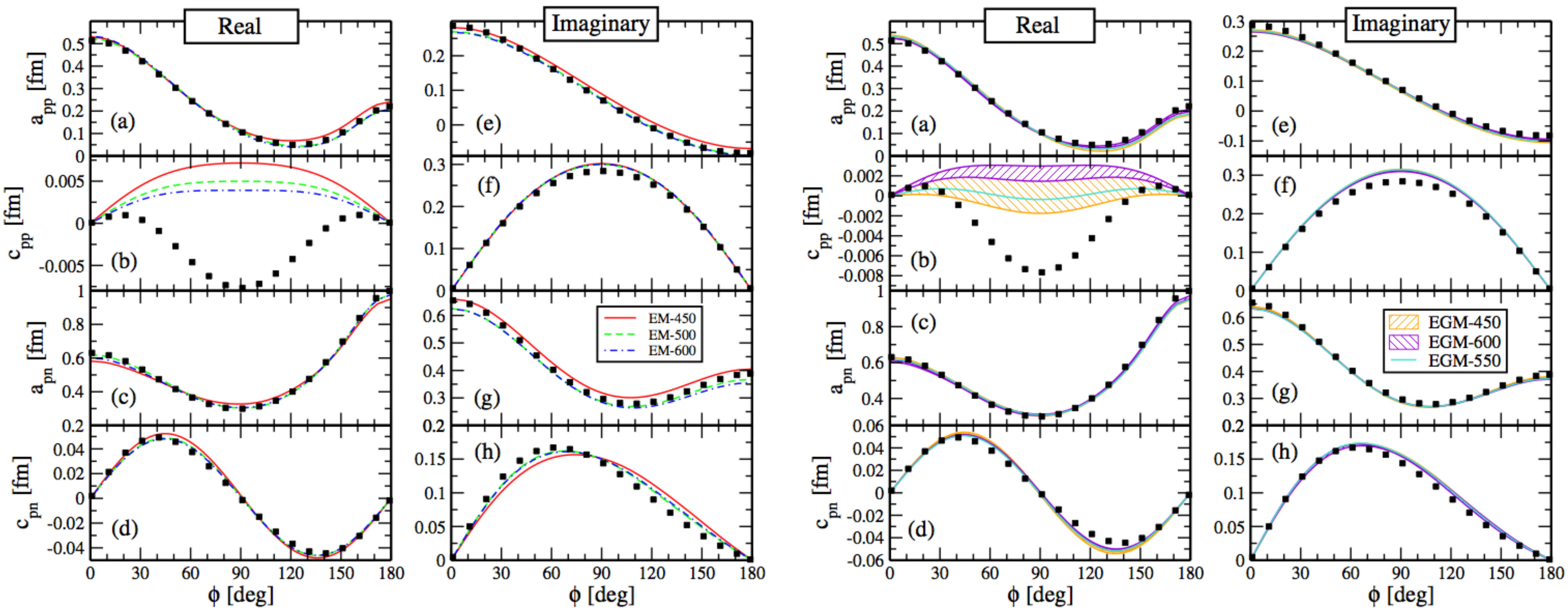

M. Vorabbi, P. Finelli, C. Giusti, PRC 93 034619 (2016)

OP and scattering observables

The most general form of the amplitude for elastic p scattering from a spin 0 nucleus

$$M(k_0,\theta) = A(k_0,\theta) + \boldsymbol{\sigma}\cdot\hat{\mathbf{N}}\,C(k_0,\theta)$$

Scattering observables

$$\frac{d\sigma}{d\Omega}(\theta) = |A(\theta)|^2 + |C(\theta)|^2$$

unpolarized differential cross section

$$A_y(\theta) = \frac{2\mathrm{Re}[A^*(\theta)\,C(\theta)]}{|A(\theta)|^2 + |C(\theta)|^2}$$

analyzing power

$$Q(\theta) = \frac{2\mathrm{Im}[A(\theta)\,C^*(\theta)]}{|A(\theta)|^2 + |C(\theta)|^2}$$

spin rotation

ELASTIC PROTON SCATTERING

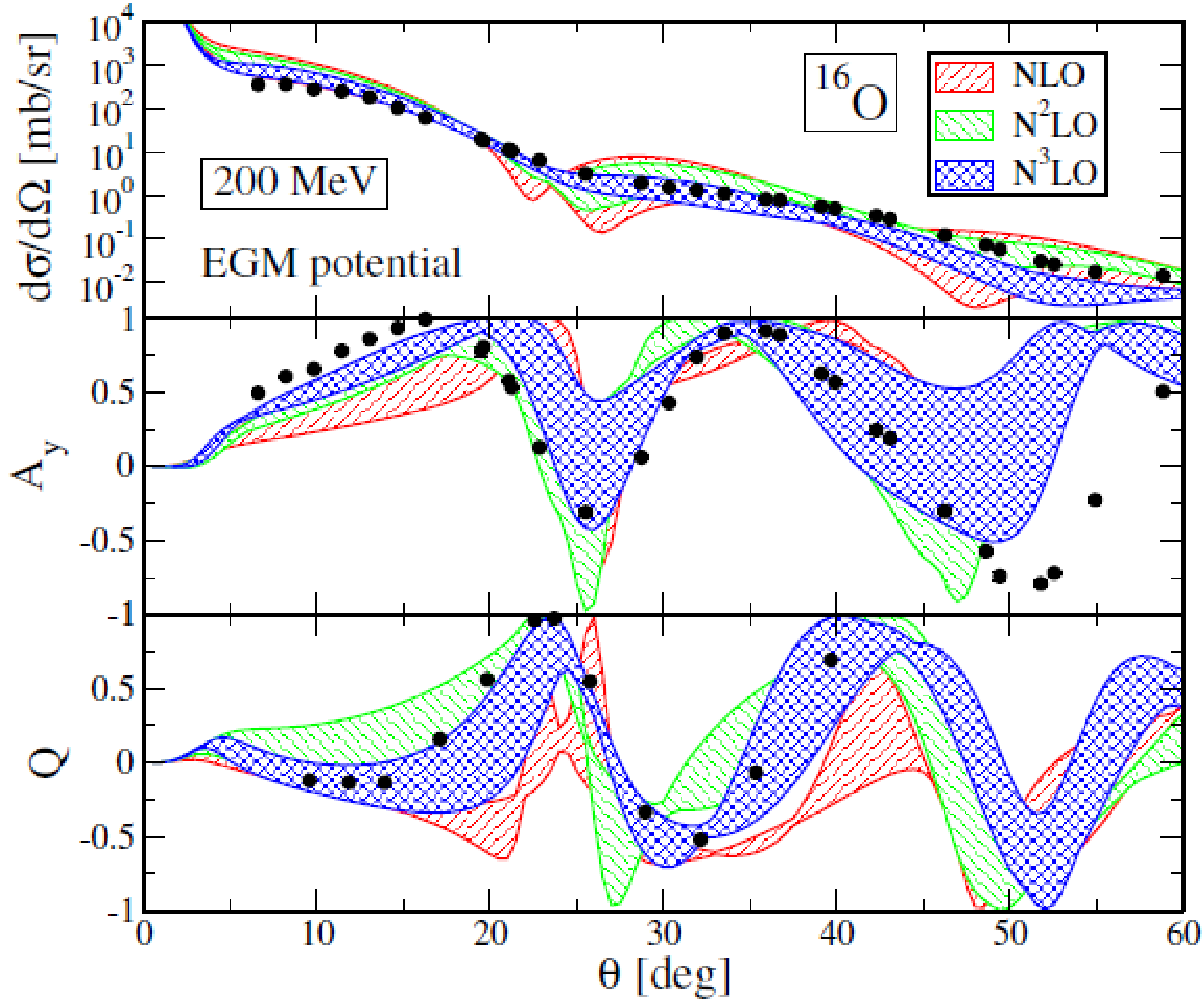

M. Vorabbi, P. Finelli, and C. Giusti, Phys. Rev. C **93**, 034619 (2016)

ELASTIC P-A SCATTERING

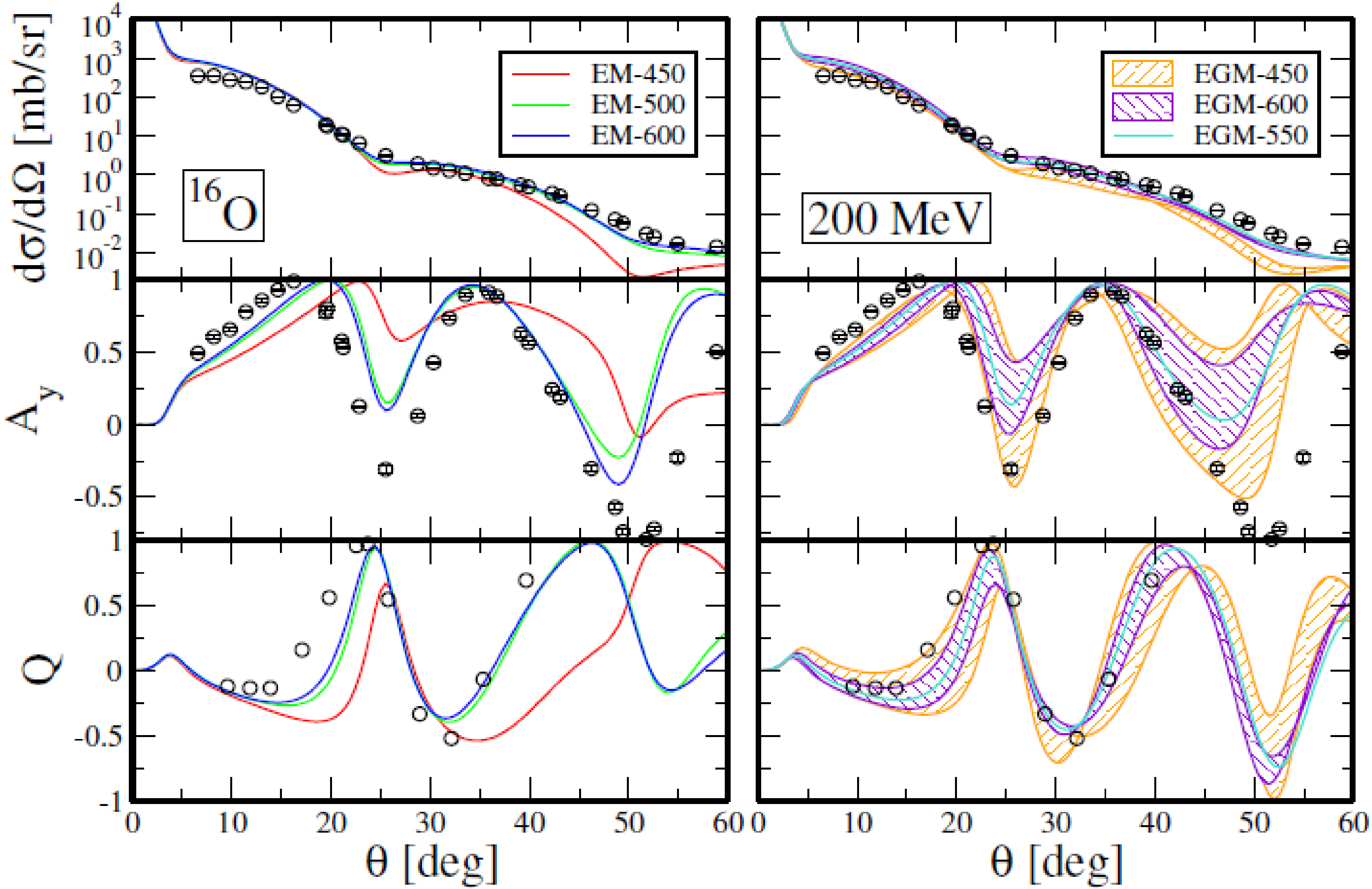

M. Vorabbi, P. Finelli, and C. Giusti, Phys. Rev. C **93**, 034619 (2016)

ELASTIC P-A SCATTERING

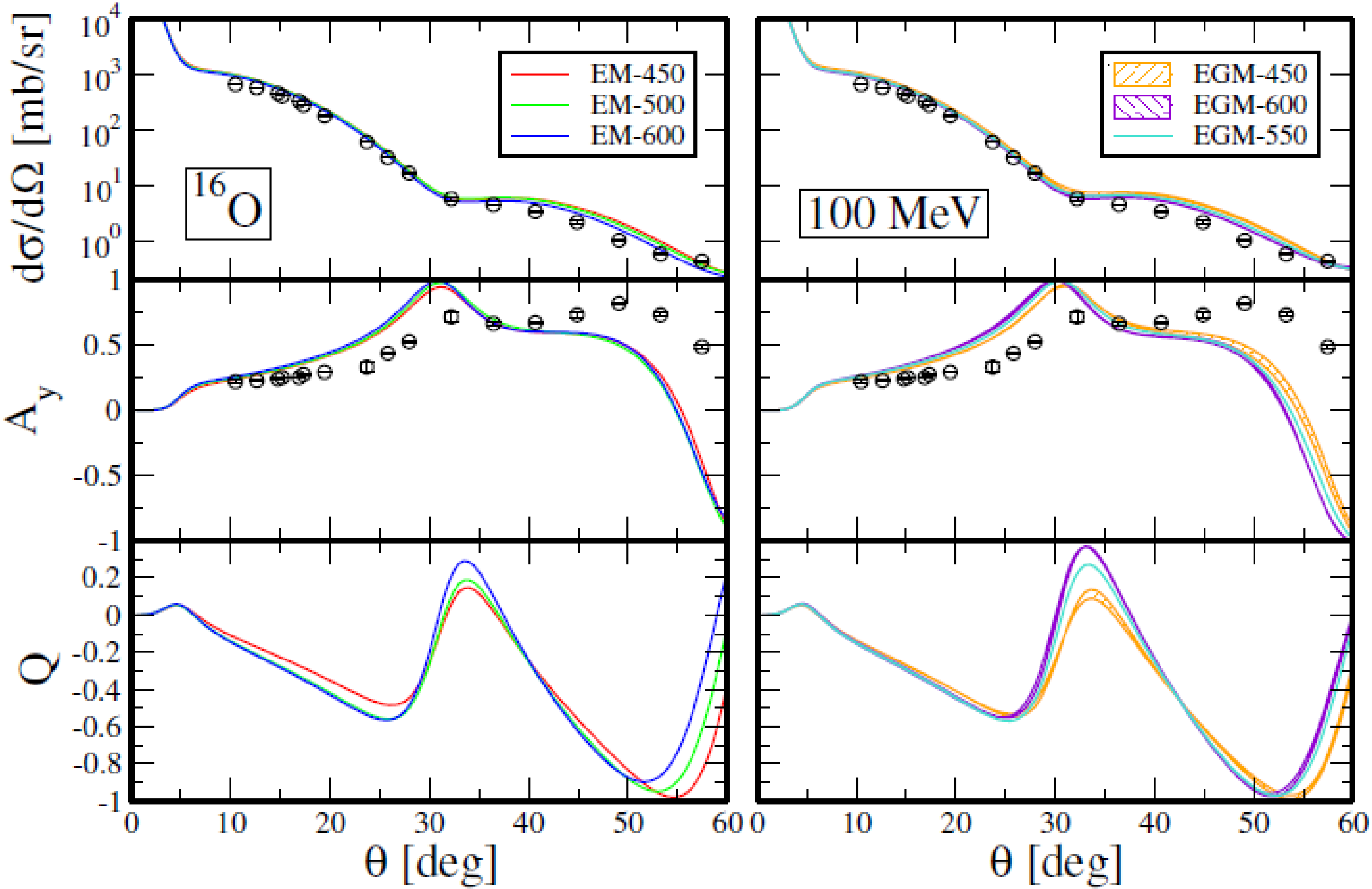

M. Vorabbi, P. Finelli, and C. Giusti, Phys. Rev. C **93**, 034619 (2016)

M. Vorabbi, P. Finelli, C. Giusti, PRC 93 034619 (2016)

Theoretical optical potential derived from nucleon-nucleon chiral potentials

M. Vorabbi, P. Finelli, C. Giusti, PRC 93 034619 (2017)

Optical potential derived from nucleon-nucleon chiral potentials at N^4LO

CHIRAL POTENTIAL AT N^4LO

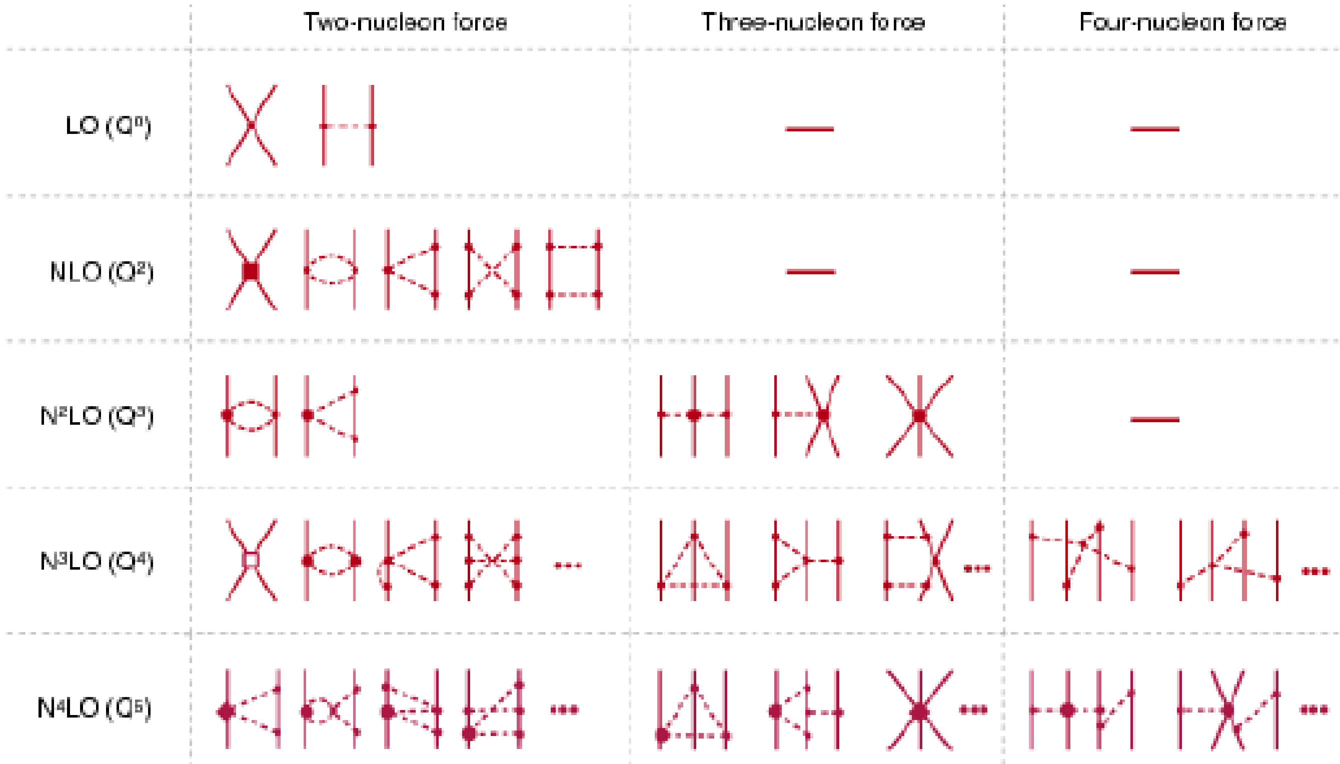

E. Epelbaum et al. . PRL 115 122391 (2015), EPJA 51 53 (2015) EKM

D.R. Entem et al. PRC 91 014002 (2015), PRC 96 024004 (2017) EMN

CHIRAL POTENTIAL AT N^{4}LO

NN

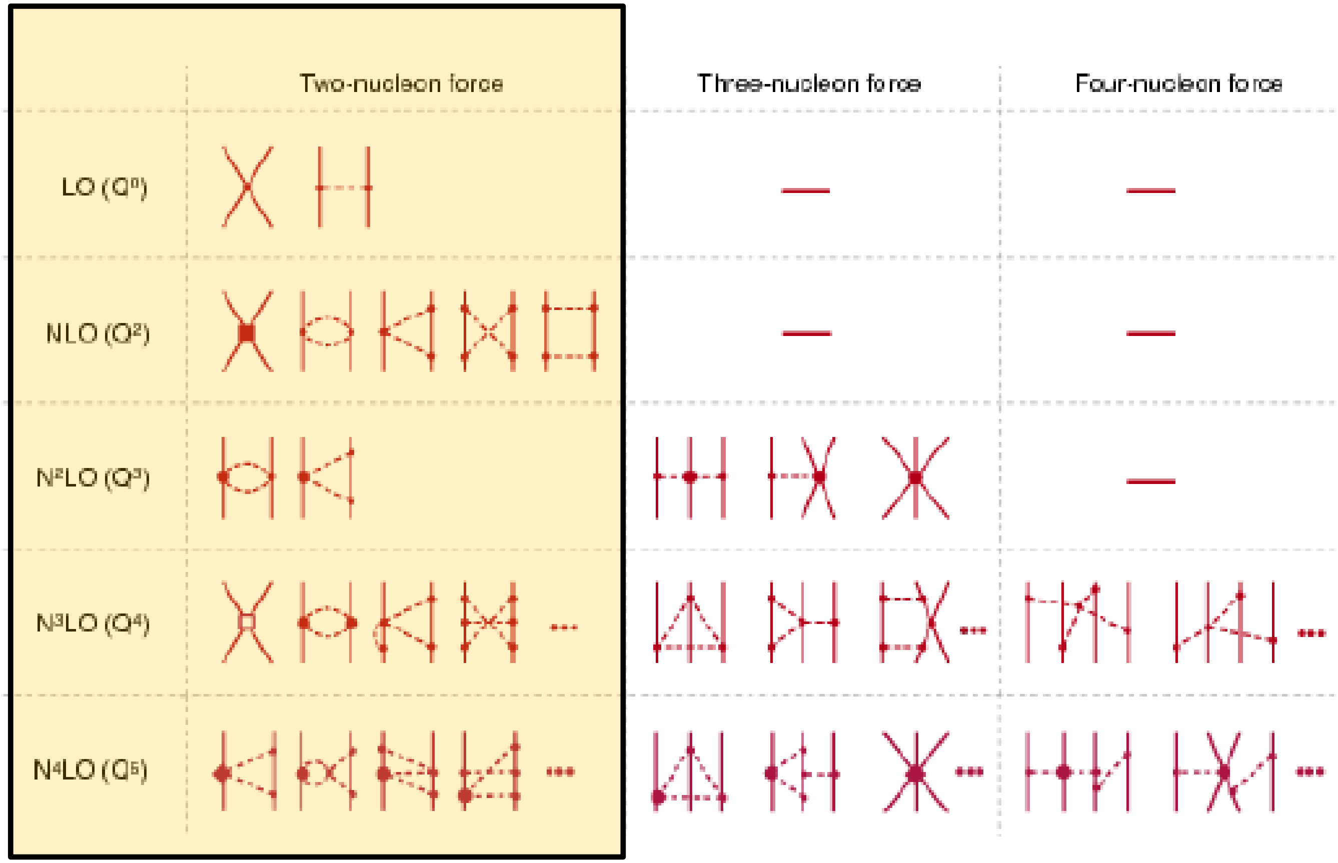

E. Epelbaum et al. . PRL 115 122391 (2015), EPJA 51 53 (2015) EKM

D.R. Entem et al. PRC 91 014002 (2015), PRC 96 024004 (2017) EMN

M. Vorabbi, P. Finelli, C. Giusti, PRC 93 034619 (2017)

Optical potential derived from nucleon-nucleon chiral potentials at N^4LO

Purpose: check the convergence and assess the theoretical errors associated with the truncation of the chiral expansion in the construction of an OP

Regularization for EKM and EMN at N^4LO

EKM

Long-range part of the potential
n=6   R=0.8, 0.9, 1., 1. 1, 1.2 fm

$$f\left(\frac{r}{R}\right) = \left(1 - \exp\left(-\frac{r^2}{R^2}\right)\right)^n$$

Short-range part
conventional mom. space

$$f_\Lambda(k', k) = \exp\left(-\left(\frac{k'}{\Lambda}\right)^{2m} - \left(\frac{k}{\Lambda}\right)^{2m}\right)$$

Λ= $2R^{-1}$ and m=2

EMN

SFR with $\tilde{\Lambda}$~ 700 MeV to regularize the loop contribution and a conventional regulator function with Λ = 450, 500, 550 MeV and m = 2, 4 for multi-pion and single-pion exchange contribution

Regularization for EKM and EMN at N^4LO

EKM

Long-range part of the potential

n=6 R=0.8, 0.9, 1., 1. 1, 1.2 fm

$$f\left(\frac{r}{R}\right) = \left(1 - \exp\left(-\frac{r^2}{R^2}\right)\right)^n$$

Short-range part
conventional mom. space

$$f_\Lambda(k', k) = \exp\left(-\left(\frac{k'}{\Lambda}\right)^{2m} - \left(\frac{k}{\Lambda}\right)^{2m}\right)$$

Λ= $2R^{-1}$ and m=2

EMN

SFR with $\tilde{\Lambda}$~ 700 MeV to regularize the loop contribution and a conventional regulator function with Λ = 450, 500, 550 MeV and m = 2, 4 for multi-pion and single-pion exchange contribution

Regularization for EKM and EMN at N^4LO

EKM

Long-range part of the potential

$$f\left(\frac{r}{R}\right) = \left(1 - \exp\left(-\frac{r^2}{R^2}\right)\right)^n$$

n=6 R=0.8, 0.9, 1., 1. 1, 1.2 fm

Short-range part
conventional mom. space

$$f_\Lambda(k', k) = \exp\left(-\left(\frac{k'}{\Lambda}\right)^{2m} - \left(\frac{k}{\Lambda}\right)^{2m}\right)$$

Λ= $2R^{-1}$ and m=2

all calculations performed with R=0.9 fm for EKM and Λ = 500 MeV for EMN

EMN

SFR with $\tilde{\Lambda}$~ 700 MeV to regularize the loop contribution and a conventional regulator function with Λ = 450, 500, 550 MeV and m = 2, 4 for multi-pion and single-pion exchange contribution

Assess theoretical errors associated to the truncation of the chiral expansion: *given an observable* $\mathcal{O}(p)$ the uncertainty at order n is *given* by the size of neglected high-order terms. At N^4LO:

$$\begin{aligned}
\Delta\mathcal{O}^{N^4LO}(p) = \max\big(& Q^6 \times |\mathcal{O}^{LO}(p)|, \\
& \times Q^4 \times |\mathcal{O}^{LO}(p) - \mathcal{O}^{NLO}(p)|, \\
& \times Q^3 |\mathcal{O}^{NLO}(p) - \mathcal{O}^{N^2LO}(p)|, \\
& \times Q^2 \times |\mathcal{O}^{N^2LO}(p) - \mathcal{O}^{N^3LO}(p)|, \\
& \times Q |\mathcal{O}^{N^3LO}(p) - \mathcal{O}^{N^4LO}(p)|\big),
\end{aligned}$$

$$Q = \max\left(\frac{p}{\Lambda_b}, \frac{M_\pi}{\Lambda_b}\right) \qquad \Lambda_b = 600\ \text{MeV}$$

NN AMPLITUDES 200 MeV

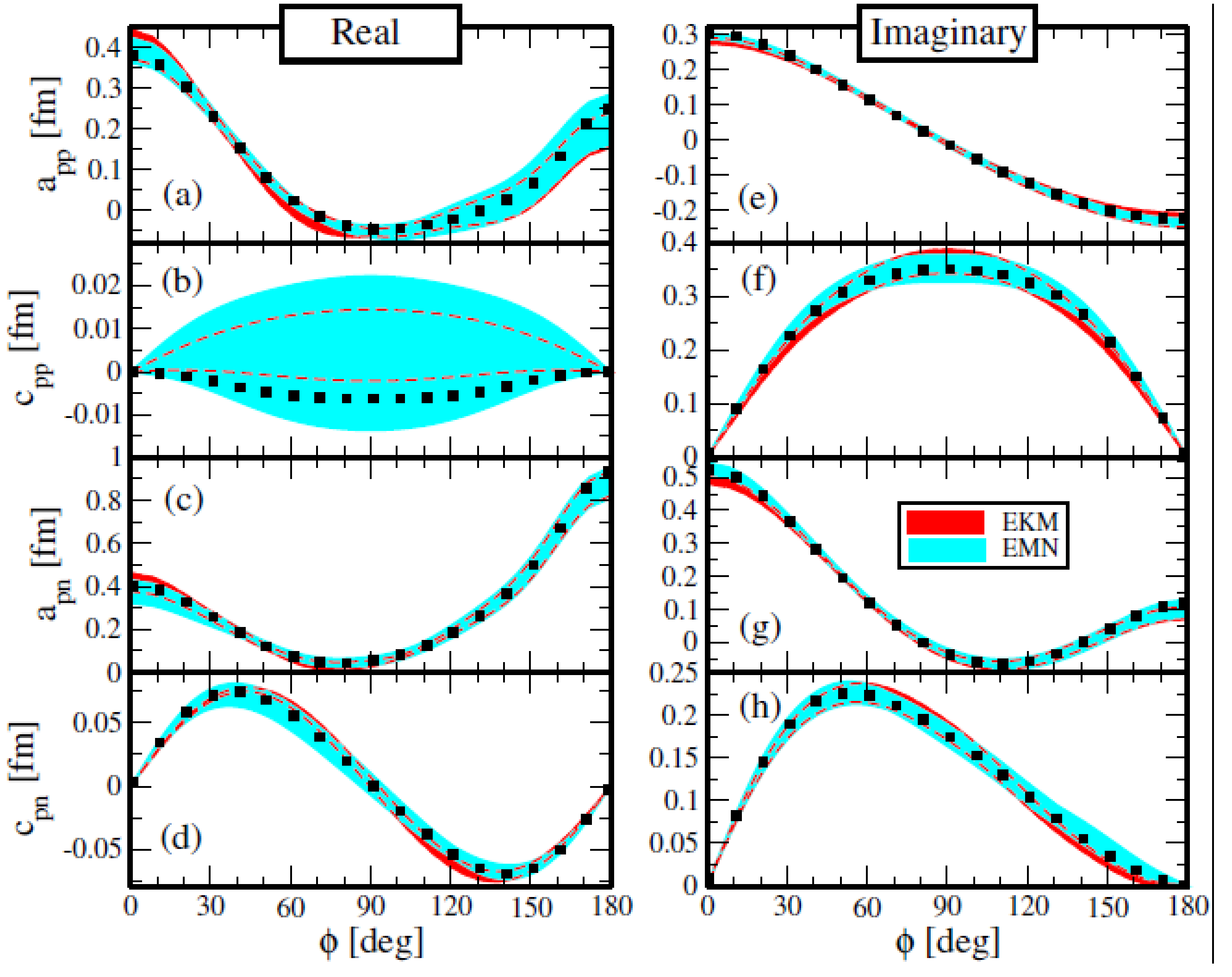

M. Vorabbi, P. Finelli, C. Giusti PRC 96 044001 (2017)

^{16}O

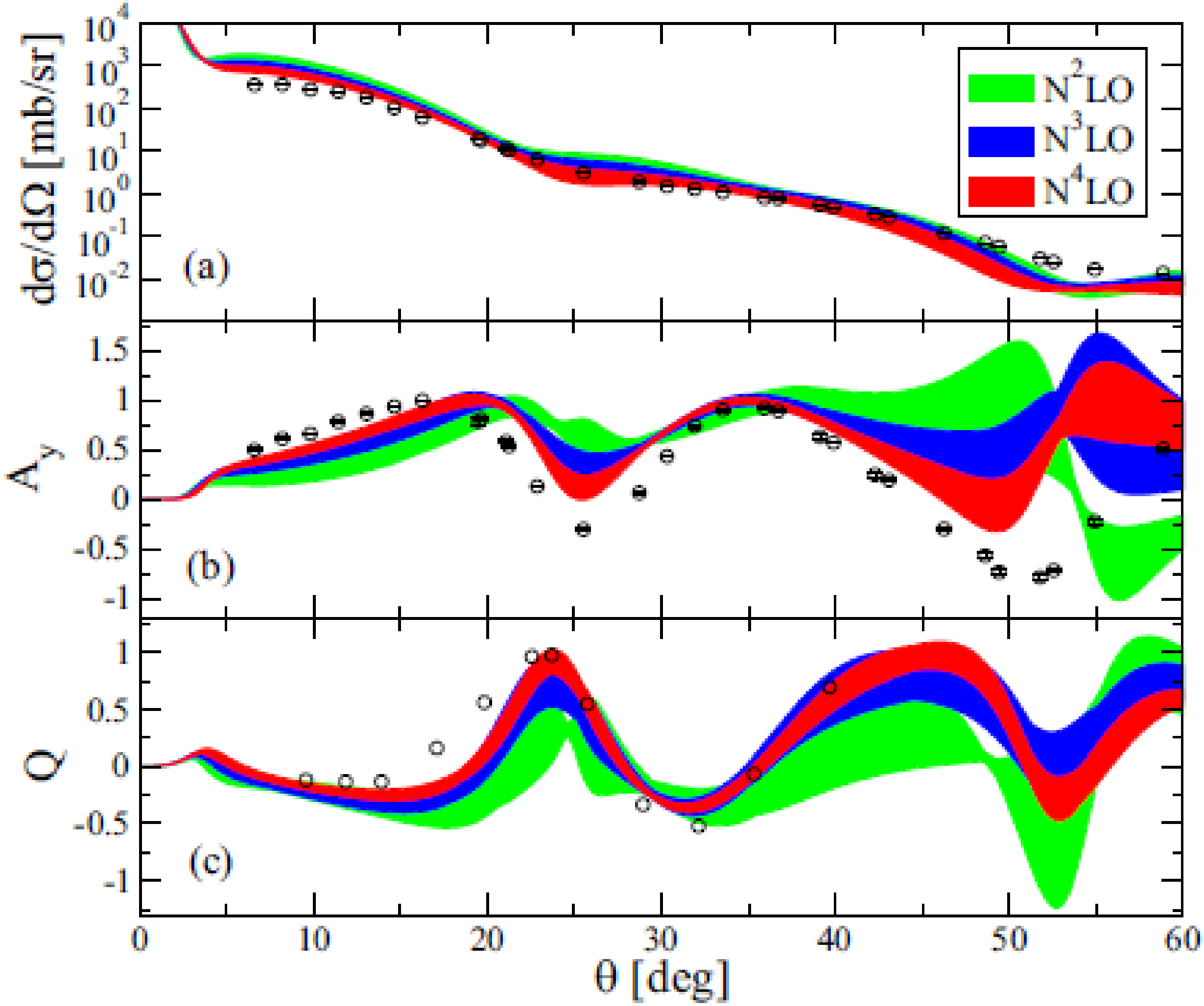

200 MeV

EKM

M. Vorabbi, P. Finelli, C. Giusti PRC 96 044001 (2017)

^{16}O 200 MeV ^{40}Ca

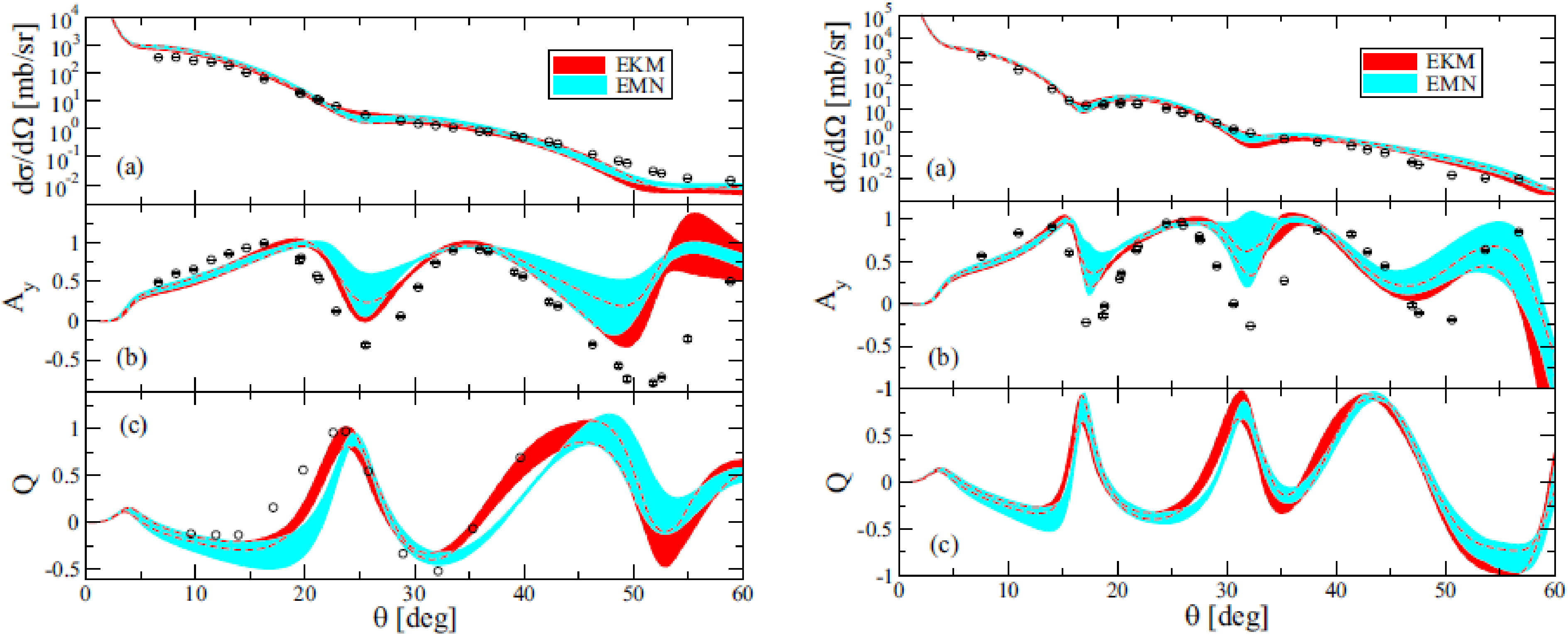

M. Vorabbi, P. Finelli, C. Giusti PRC 96 044001 (2017)

Comparison with phenomenological OP

- investigate and compare predictive power of our microscopic OP and of phenomenological OP in comparison with exp. data in a wider range of nuclei, including isotopic chains

PHENOMENOLOGICAL OP
parameters fitted to data,
data very well described in particular situations.
Investigate capability to describe data in different situations

MICROSCOPIC OP
obtained from a model and approximations
may be less able to describe specific data
should have a greater predictive power for situations for which data not yet available

Comparison phenomenological and microscopic NROP

PHENONOMENOLOGICAL OP

GLOBAL given in a wide range of nuclei and energies

NROP up to ~200 MeV, for higher energies it is generally believed that the Schroedinger picture should be taken over by a Dirac approach. Global ROP available up to ~1 GeV

NROP Koning at al. NPA 713 231 (2003) (KON) for nuclei $24 \leqslant A \leqslant 209$ and energies from 1 keV to 200 MeV, recently extended to 1 GeV, to test at which energy the predictions of a phen. NROP fail

Calculations with TALYS (ECIS-06)

MICROSCOPIC OP
chiral potentials at N^4LO describe NN scattering data up to 300 MeV and our OP can be used up to ~ 300 MeV

Comparison phenomenological and microscopic NROP

PHENONOMENOLOGICAL OP

GLOBAL given in a wide range of nuclei and energies

NROP up to ~200 MeV, for higher energies it is generally believed that the Schroedinger picture should be taken over by a Dirac approach. Global ROP available up to ~1 GeV

NROP Koning at al. NPA 713 231 (2003) (KON) fo
and energies fro
recently extende
at which energy t
phen. NROP fail

Calculations with TALYS (ECIS-06)

MICROSCOPIC OP
chiral potentials at N^{4}LO describe NN scattering data up to 300 MeV and our OP can be used up to ~ 300 MeV

Results of the comparison in the energy range 150-330 MeV

Comparison phenomenological and microscopic NROP

PHENONOMENOLOGICAL OP

GLOBAL given in a wide range of nuclei and energies

NROP up to ~200 MeV, for higher energies it is generally believed that the Schroedinger picture should be taken over by a Dirac approach. Global ROP available up to ~1 GeV

NROP Koning a
(2003) (KON)
and energies f
recently exten
at which energy the predictions of a phen. NROP fail

Calculations with TALYS (ECIS-06)

MICROSCOPIC OP
chiral potentials at N^4LO describe NN scattering data up to 300 MeV and our OP can be used up to ~ 300 MeV

calculations with R=0,8,0.9,1. fm (EKM)
Λ=500,550 MeV (EMN)
The bands give the differences

Comparison with phenomenological OP

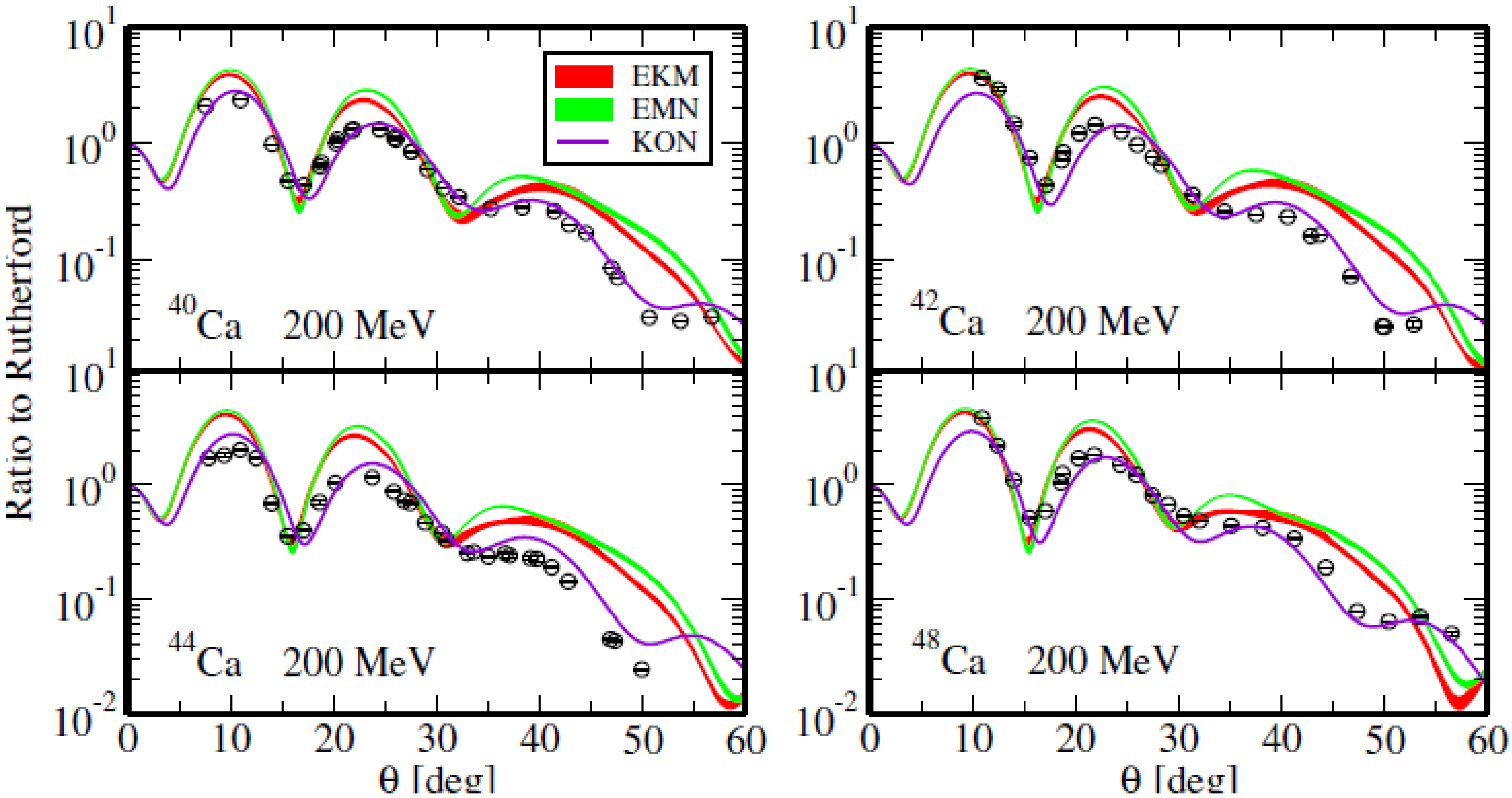

Comparison with phenomenological OP

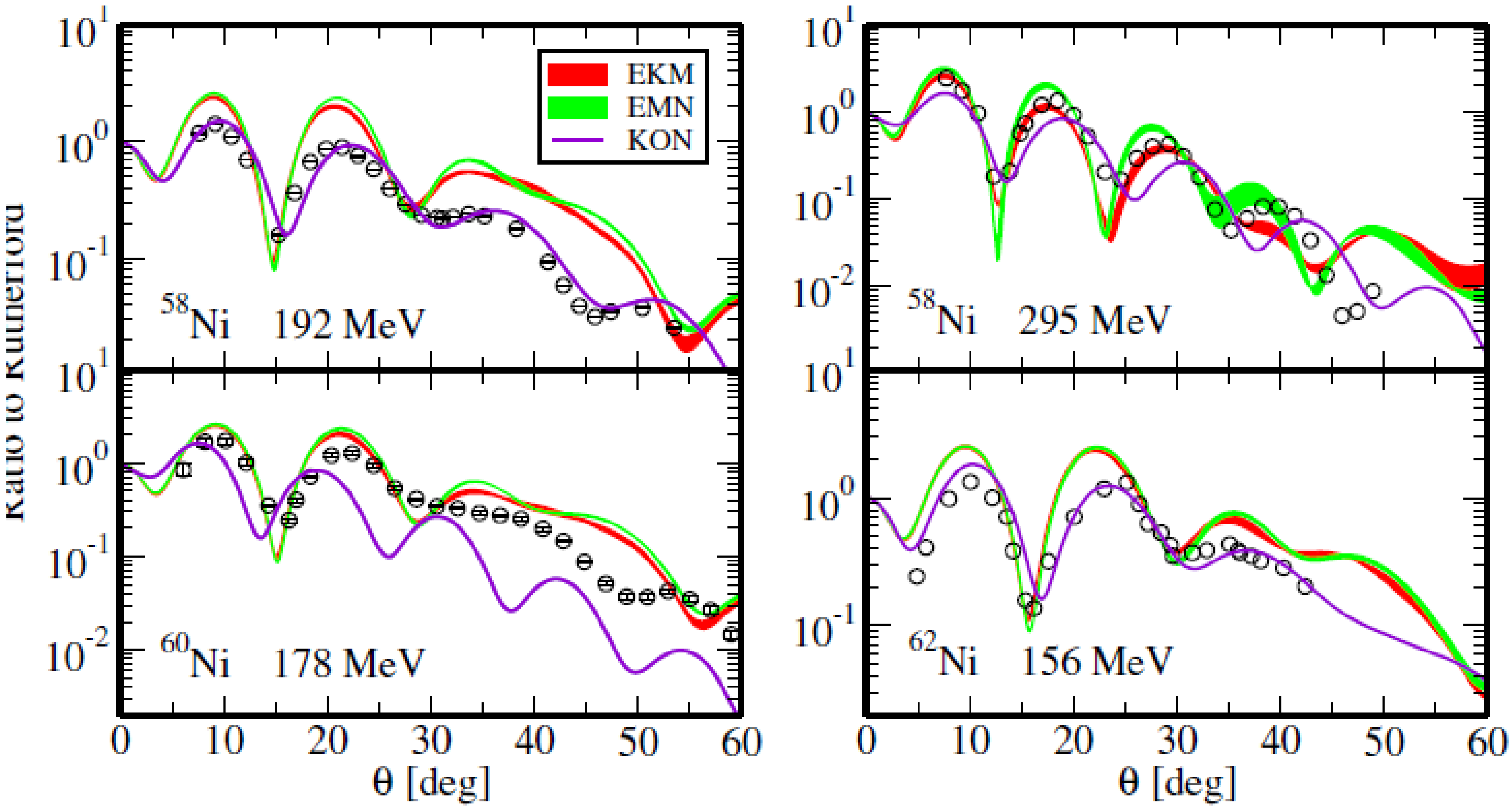

Comparison with phenomenological OP

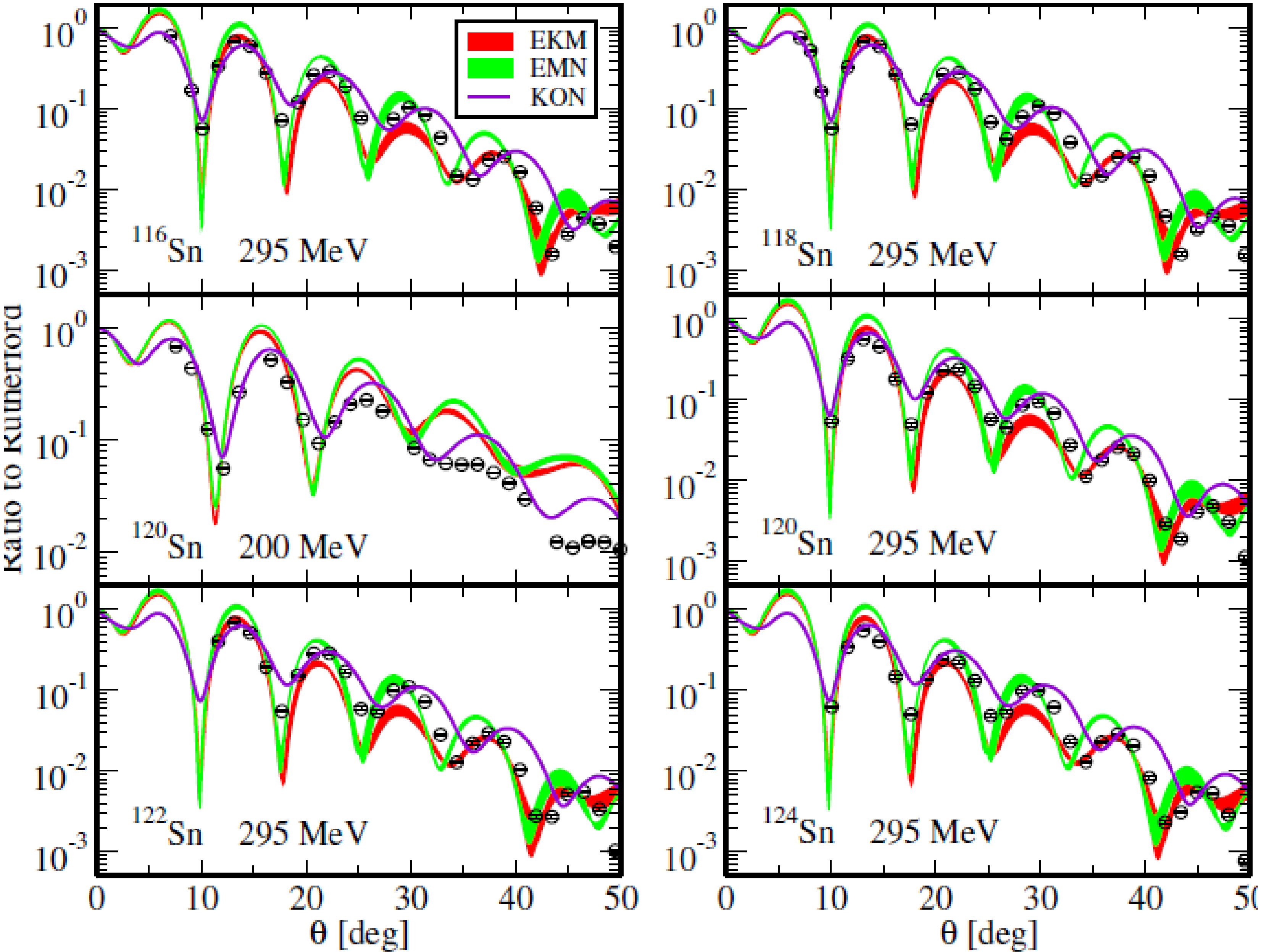

Comparison with phenomenological OP

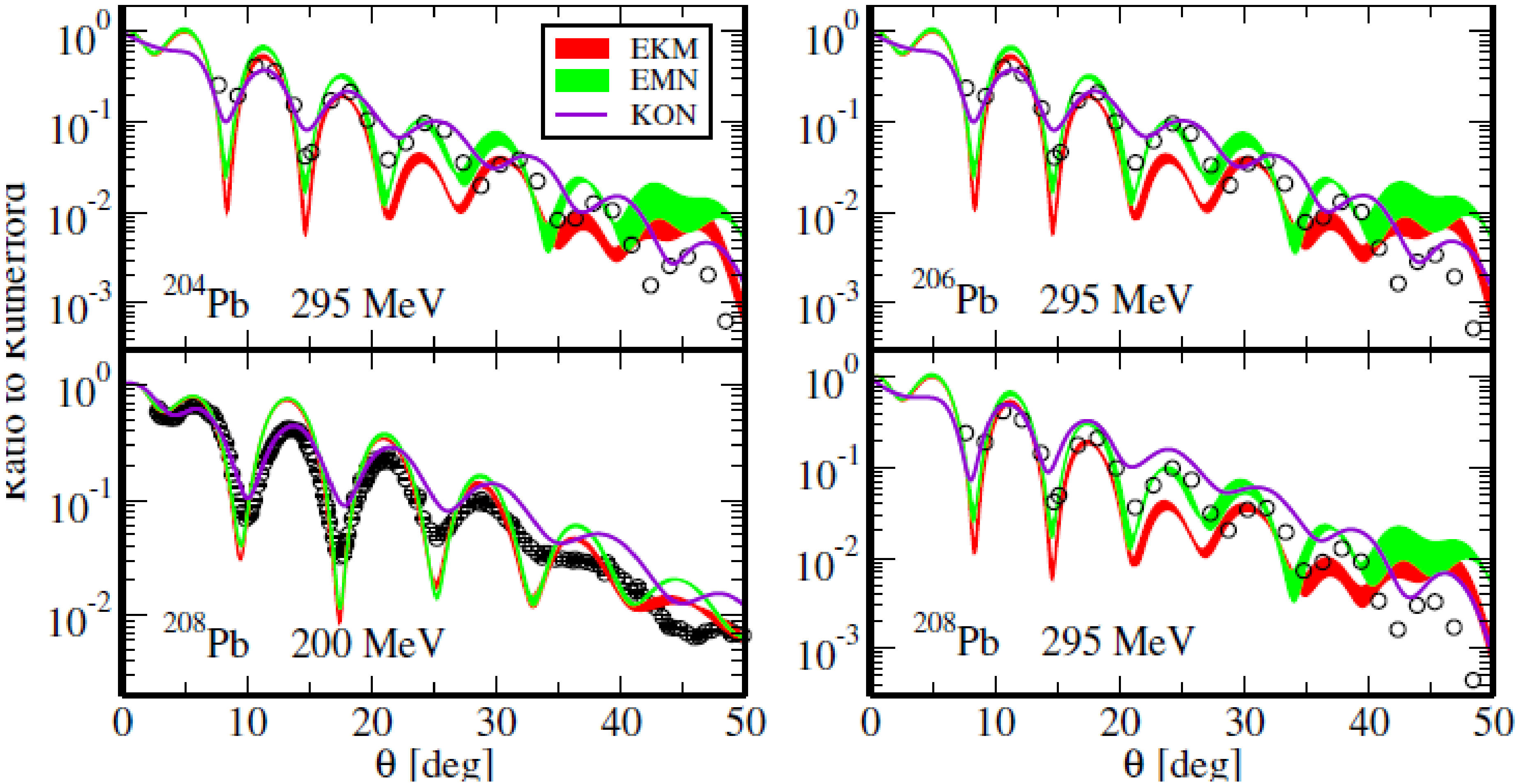

Comparison with phenomenological OP

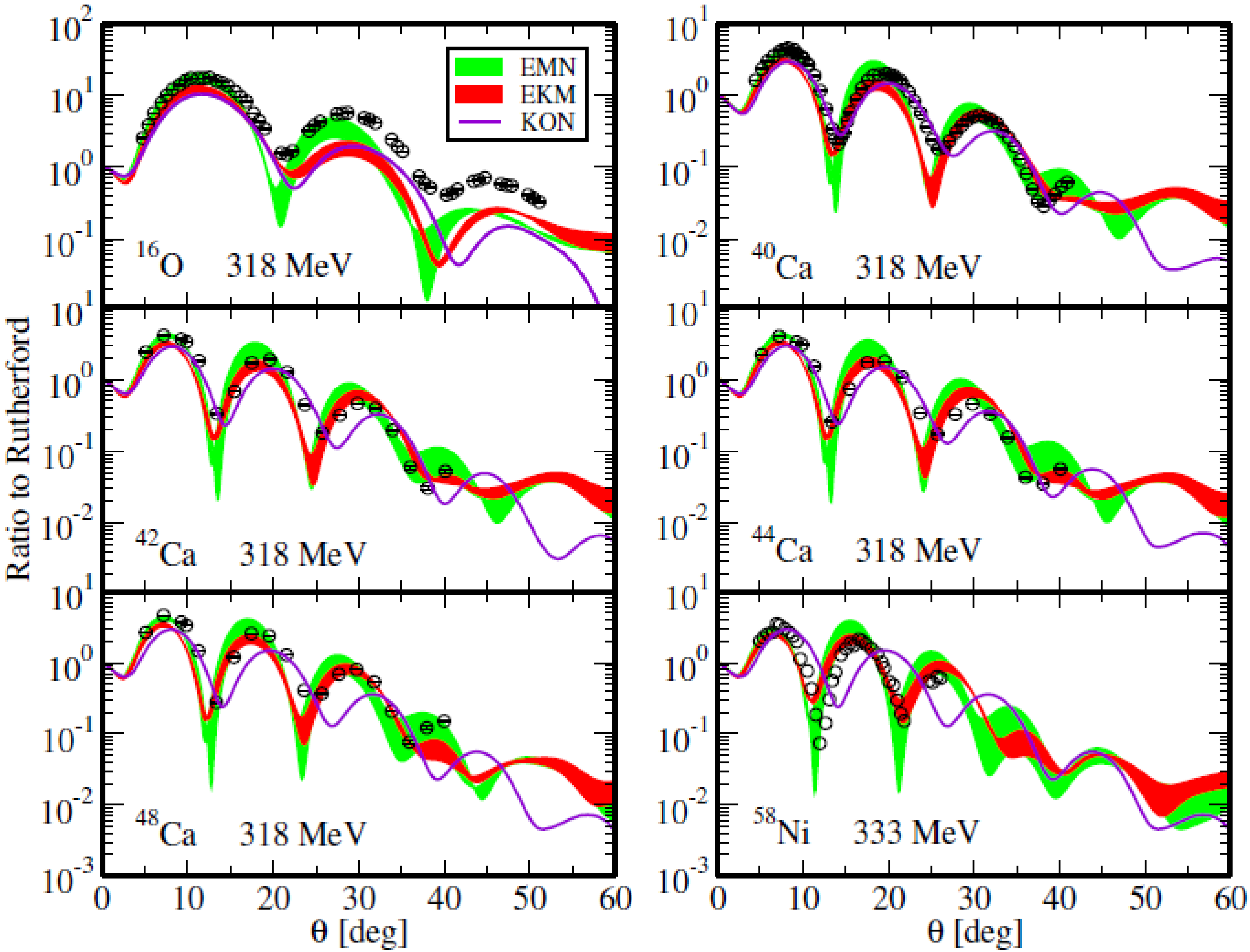

Comparison with phenomenological OP

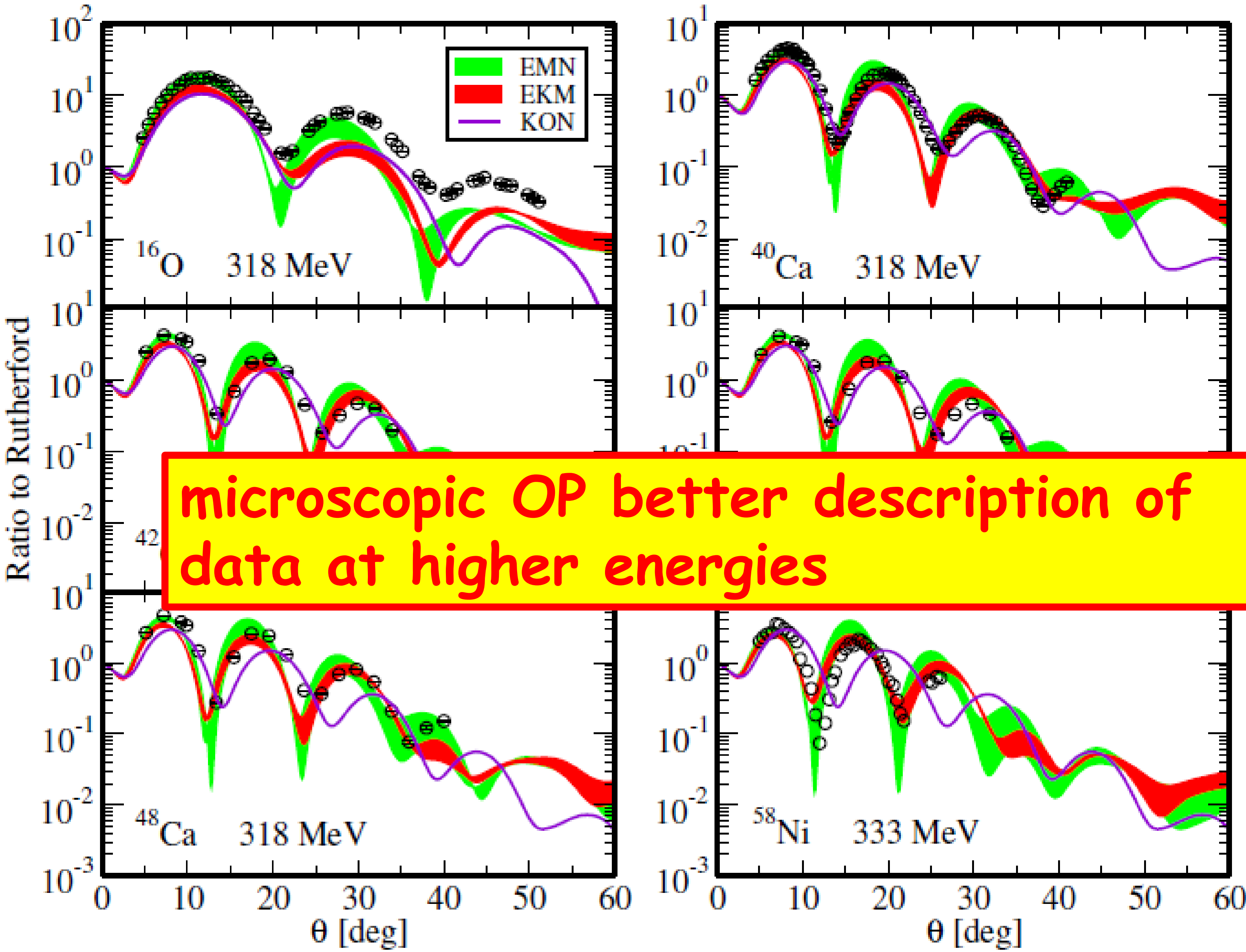

microscopic OP better description of data at higher energies

PROSPECTS...

- model can be improved

Microscopic optical potentials derived from *ab initio* translationally invariant nonlocal one-body densities

Michael Gennari*
University of Waterloo, 200 University Avenue West Waterloo, Ontario N2L 3G1, Canada
TRIUMF, 4004 Wesbrook Mall, Vancouver, British Columbia V6T 2A3, Canada

Matteo Vorabbi,† Angelo Calci, and Petr Navrátil‡
TRIUMF, 4004 Wesbrook Mall, Vancouver, British Columbia V6T 2A3, Canada
(Dated: December 11, 2017)

Background: The nuclear optical potential is a successful tool for the study of nucleon-nucleus elastic scattering and its use has been further extended to inelastic scattering and other nuclear reactions. The nuclear density of the target nucleus is a fundamental ingredient in the construction of the optical potential and thus plays an important role in the description of the scattering process.
Purpose: In this work we derive a microscopic optical potential for intermediate energies using *ab initio* translationally invariant nonlocal one-body nuclear densities computed within the no-core shell model (NCSM) approach utilizing two- and three-nucleon chiral interactions as the only input.
Methods: The optical potential is derived at first-order within the spectator expansion of the non-relativistic multiple scattering theory by adopting the impulse approximation. Nonlocal nuclear densities are derived from the NCSM one-body densities calculated in the second quantization. The translational invariance is generated by exactly removing the spurious center-of-mass (COM) component from the NCSM eigenstates.
Results: The ground state local and nonlocal densities of ^{4,6,8}He, ^{12}C, and ^{16}O are calculated and applied to optical potential construction. The differential cross sections and the analyzing powers for the elastic proton scattering off of these nuclei are then calculated for different values of the incident proton energy. The impact of nonlocality and the COM removal is discussed.
Conclusions: The use of nonlocal densities has a substantial impact on the differential cross sections and improves agreement with experiment in comparison to results generated with the local densities especially for light nuclei. For the halo nuclei ^{6}He and ^{8}He, the results for the differential cross section are in a reasonable agreement with the data although a more sophisticated model for the optical potential is required to properly describe the analyzing powers.

PACS numbers: 24.10.-i; 24.10.Ht; 24.70.+s; 25.40.Cm;21.60.De;27.10.+h;27.20.+n

M. Gennari, M. Vorabbi, A. Calci, P. Navratil, arXiv: 1712.02879 (2017)

PROSPECTS...

- the model can be improved
- folding integral
- 3N forces, medium effects
- application to nuclear reactions.... ? (e,e'p)